Department of Forest Products Technology

Wood biomass characterization by Raman spectroscopy

Anni Lähdetie

Aalto University

DOCTORAL DISSERTATIONS

Aalto University publication series
DOCTORAL DISSERTATIONS 202/2013

Wood biomass characterization by Raman spectroscopy

Anni Lähdetie

A doctoral dissertation completed for the degree of Doctor of Science (Technology) to be defended, with the permission of the Aalto University School of Chemical Technology, at a public examination held at the auditorium of the Department of Forest Products Technology on 11 December 2013 at 12.

Aalto University
School of Chemical Technology
Department of Forest Products Technology
Forest Products Chemistry

Supervising professor
Professor Tapani Vuorinen

Thesis advisor
Dr. Anna-Stiina Jääskeläinen

Preliminary examiners
Associate Professor Christine Chirat, Grenoble INP-Pagora, France
Dr.rer.nat. Notburga Gierlinger, BOKU, Austria

Opponent
Associate Professor Søren Barsberg, University of Copenhagen, Denmark

Aalto University publication series
DOCTORAL DISSERTATIONS 202/2013

ISBN 978-952-60-5468-1
ISBN 978-952-60-5469-8 (pdf)
ISSN-L 1799-4934
ISSN 1799-4934 (printed)
ISSN 1799-4942 (pdf)
http://urn.fi/URN:ISBN:978-952-60-5469-8

http://lib.tkk.fi/Diss/

Unigrafia Oy
Helsinki 2013

Finland

441 697
Printed matter

Aalto University

Abstract

Aalto University, P.O. Box 11000, FI-00076 Aalto www.aalto.fi

Author
Anni Lähdetie

Name of the doctoral dissertation
Wood biomass characterization by Raman spectroscopy

Publisher School of Chemical Technology

Unit Department of Forest Products Technology

Series Aalto University publication series DOCTORAL DISSERTATIONS 202/2013

Field of research Forest Products Chemistry

Manuscript submitted 16 October 2012 **Date of the defence** 11 December 2013

Permission to publish granted (date) 18 December 2012 **Language** English

☐ **Monograph** ☒ **Article dissertation (summary + original articles)**

Abstract

Lignin is nature's second most abundant polymer after cellulose. However, many uncertainties still remain about the structure, formation, and reactions of lignin as well as its distribution in plant cells. The analysis of the lignin structure is challenging, and the isolation of lignin from biomass introduces changes, regardless of the isolation method applied.

In order to be able to utilize lignin efficiently and sustainably, potent analytical techniques are needed. Raman spectroscopy is a nondestructive technique that is applicable to characterize wood biomass in situ. The objective of this research was to utilize Raman spectroscopy in wood biomass research, especially in the analysis of the structure and reactions of lignin.

To obtain a more detailed understanding of applicability of Raman spectroscopy in bleaching studies, unbleached and bleached kraft pulps were analyzed. Furthermore, chemical changes in thermomechanical pulp (TMP) during enzymatic treatment were monitored. UV resonance Raman (UVRR) spectroscopy was shown to be a valuable technique in lignin analysis in situ, especially for pulp samples with a low lignin content. Monitoring small changes in TMP samples with a high lignin content using Raman spectroscopy proved to be challenging, as the resonance enhancement of the aromatic band became very strong.

To develop the quantitative Raman spectroscopic analysis method for phenolic hydroxyl group determination, the effect of pH on lignin analysis was investigated using lignin model compounds and wood pulps. UVRR spectroscopy was shown to be equally applicable to samples with a high lignin content and those with a very low lignin content.

Raman spectroscopy of lignin-containing samples may produce laser induced fluorescence which overlaps with Raman bands. The fluorescence properties of the lignin model compounds were studied. Lignin model compounds containing a biphenyl structure exhibited strong laser induced fluorescence with visible excitation in Raman spectroscopy. Wood did not emit laser induced fluorescence, but when it was chemically treated under alkaline conditions, considerable amount of fluorescence was detected in the Raman spectrum.

The effect of excitation wavelength on the Raman spectra of wood-based samples was investigated. Several lasers were used to obtain excitation ranging from ultraviolet to near infrared radiation to see how the different laser frequencies affected the Raman spectra of wood biomass samples. The intensities of the characteristic vibration bands of different structural features in the Raman spectra of wood-based samples were shown to depend on the excitation wavelength.

Keywords lignin, pulp, wood biomass, Raman spectroscopy

ISBN (printed) 978-952-60-5468-1 **ISBN (pdf)** 978-952-60-5469-8

ISSN-L 1799-4934 **ISSN (printed)** 1799-4934 **ISSN (pdf)** 1799-4942

Location of publisher Espoo **Location of printing** Helsinki **Year** 2013

Pages 148 **urn** http://urn.fi/URN:ISBN:978-952-60-5469-8

A! Aalto-yliopisto

Tiivistelmä

Aalto-yliopisto, PL 11000, 00076 Aalto www.aalto.fi

Tekijä
Anni Lähdetie

Väitöskirjan nimi
Puubiomassan karakterisointi ramanspektroskopialla

Julkaisija Kemian tekniikan korkeakoulu

Yksikkö Puunjalostustekniikan laitos

Sarja Aalto University publication series DOCTORAL DISSERTATIONS 202/2013

Tutkimusala Puunjalostuksen kemia

Käsikirjoituksen pvm 16.10.2012 **Väitöspäivä** 11.12.2013

Julkaisuluvan myöntämispäivä 18.12.2012 **Kieli** Englanti

☐ **Monografia** ☒ **Yhdistelmäväitöskirja (yhteenveto-osa + erillisartikkelit)**

Tiivistelmä

Ligniini on selluloosan jälkeen toiseksi yleisin luonnosta löytyvä polymeeri. Kuitenkaan ligniinin rakenteesta, reaktioista tai sen sijainnista kasvisoluissa ei vieläkään tiedetä kaikkea. Ligniinin kemiallinen analysointi on haasteellista, sillä ligniinin eristäminen puubiomassasta aiheuttaa aina muutoksia sen rakenteeseen.

Jotta ligniiniä voitaisiin hyödyntää paremmin teollisuudessa, tarvitaan tehokkaita analyysimenetelmiä sen tutkimiseksi. Ramanspektroskopia on analyysimenetelmä, joka ei edellytä tutkittavien komponenttien eristämistä, joten ligniiniä voidaan tutkia alkuperäisessä ympäristössään (in situ). Tämän työn tarkoituksena oli tutkia ramanspektroskopian hyödyntämistä puubiomassan tutkimuksessa.

Valkaisemattomia ja valkaistuja sulfaattimassoja analysoitiin ultravioletti-resonanssi ramanspektroskopialla (UVRR-spektroskopialla) sellun valkaisukemian tutkimiseksi. Menetelmällä monitoroitiin myös entsyymikäsittelyn aiheuttamia kemiallisia muutoksia mekaanisessa massassa (TMP). UVRR-spektroskopian havaittiin olevan tehokas analyysimenetelmä erityisesti niille näytteille, joiden ligniinipitoisuus oli pieni. Toisaalta pienten muutosten havainnointi UVRR-spektroskopialla osoittautui haastavaksi paljon ligniiniä sisältävien näytteiden kohdalla (erityisesti TMP) voimakkaan resonanssivahvistumisen takia.

Malliaineiden avulla tutkittiin pH:n vaikutusta ligniinin fenolisten hydroksyyliryhmien määrittämiseen ramanspektroskopialla. UVRR-spektroskopian osoitettiin olevan hyvä analyysimenetelmä sekä paljon että vähän ligniiniä sisältäville näytteille.

Ramanspektroskopiamenetelmän eräs suurimmista heikkouksista on virittävän laserin aikaansaama fluoresenssi, joka voi peittää ligniinipitoisesta näytteestä tulevan ramansignaalin täysin. Ligniinin fluoresenssia ramanspektroskopiassa tutkittiin erilaisten malliaineiden avulla, ja ligniinin bifenyylirakenteiden havaittiin fluoresoivan voimakkaasti näkyvällä valolla viritettäessä. Puunäyte ei fluoresoinut ramanspektroskopialla analysoitaessa, mutta alkalikäsitellyt puunäytteet fluoresoivat jo huomattavan paljon.

Virittävän valon aallonpituuden vaikutusta ramanspektreihin tutkittiin puubiomassanäytteillä. Useita erilaisia lasereita käytettiin virittämään näytteitä ultraviolettialueelta lähi-infrapuna-alueelle. Eri puubiomassan rakenteiden vahvistuminen ramanspektrissä havaittiin olevan riippuvainen virittävästä aallonpituudesta.

Avainsanat ligniini, puubiomassa, sellu, ramanspektroskopia

ISBN (painettu) 978-952-60-5468-1 **ISBN (pdf)** 978-952-60-5469-8

ISSN-L 1799-4934 **ISSN (painettu)** 1799-4934 **ISSN (pdf)** 1799-4942

Julkaisupaikka Espoo **Painopaikka** Helsinki **Vuosi** 2013

Sivumäärä 148 **urn** http://urn.fi/URN:ISBN:978-952-60-5469-8

Preface

The research work presented in this thesis was completed during the years 2005-2012 at the Aalto University School of Chemical Technology (formerly Helsinki University of Technology). The financial support for this work from the Academy of Finland is gratefully acknowledged.

I want to thank the supervisor of this thesis, Professor Tapani Vuorinen, for giving me the opportunity to work in his research group at the Department of Forest Products Technology.

I am greatly indebted to my instructor, Dr. Anna-Stiina Jääskeläinen, for her guidance and support during all these years. Although the physical distance between us was mostly long as we were in different countries or at different workplaces, I knew I could always ask her anything, and each time I got an answer immediately. I was always "Tiina's doctoral student", and I am grateful that I was able to have her as my instructor for all this time. Also my other instructors and co-authors, Dr. Tarja Tamminen and Dr. Tiina Liitiä at VTT, were invaluable supporters and teachers to a new doctoral student like me, and later on as well. Tiina, Tarja and Tiina, thank you for everything!

My other co-authors are also thanked for their contribution to these publications. Dr. Jaana Suviniitty is thanked for checking the English language of this thesis.

I want to thank all my co-workers for creating the supportive atmosphere at Puu1 and Puu2. Rita Hatakka and Antti Kivioja are thanked for their assistance with the Raman instruments at the Department of Forest Products Technology. Taina Korhonen is thanked for her assistance with the UV-Vis spectrometer at VTT.

Members of "Teh Band" at the Department of Forest Products Technology are gratefully acknowledged for giving me an opportunity to play inspiring music that usually could not be described using words. You'd have to listen to "Villihevosia" in order to understand. Polyteknikkojen Orkesteri (the Polytech Orchestra) is thanked for giving me an opportunity to play the other kind of music as well, and for providing me "a home" during my years in Otaniemi.

I want to thank all my friends for your friendship! Dr. Tiina Komulainen and Dr. Pia Saari: Could you have guessed back in the days that despite all the hazardous Bunsen burner experiments performed at the first year student lab of Analytical Chemistry we would all become D. Sc. (Tech.) at some point…?

I am grateful to my parents and my sisters for their unconditional love and encouragement. My husband Artturi and our children Aarne and Heta are thanked for bringing happiness to my life - every day.

Espoo, November 2013
Anni Lähdetie

List of publications

This thesis is mainly based on the results presented in five publications which are referred as Roman numerals in the text.

Paper I

Lähdetie, A., Liitiä, T., Tamminen, T. and Jääskeläinen, A.-S. (2009) Reflectance UV-Vis and UV resonance Raman spectroscopy in characterization of kraft pulps, *BioResources* 4(4), 1600-1619.

Paper II

Lähdetie, A., Liitiä, T., Tamminen, T., Pere, J. and Jääskeläinen, A.-S. (2009) Activation of thermomechanical pulp by laccases as studied by UV-Vis, UV resonance Raman and FTIR spectroscopy, *Holzforschung*, 63, 745–750.

Paper III

Warsta, E., Lähdetie, A., Jääskeläinen, A.-S. and Vuorinen, T. (2012) Effect of pH on lignin analysis by Raman spectroscopy, *Holzforschung*, 66, 451–457.

Paper IV

Lähdetie, A., Nousiainen, P., Sipilä, J. Tamminen, T., and Jääskeläinen, A.-S. (2013) Laser-induced fluorescence (LIF) of lignin and lignin model compounds in Raman spectroscopy, *Holzforschung*, 67, 531-538.

Paper V

Lähdetie, A., Loureiro, P., Evtuguin, D., Sevastyanova, O., Ek, M. and Jääskeläinen, A.-S. (2013) Effect of excitation wavelength on the Raman spectra of wood-based samples (submitted).

Author's contribution:

I, II, IV, V Anni Lähdetie was responsible for the experimental design, performed the experimental work, analyzed the corresponding results, and wrote the manuscripts.

III Anni Lähdetie was partly responsible for the experimental design and the analysis of the corresponding results.

List of key abbreviations

D	chlorine dioxide stage
E	alkaline extraction stage
EMAL	enzymatic mild acidolysis lignin
FT	Fourier transform
FTIR	Fourier transform infrared
G	guaiacyl
H	*p*-hydroxyphenyl
HexA	hexenuronic acid
IR	infrared
LS	low sulphidity
MaL	*Melanocarpus albomyces* laccase
MWL	milled wood lignin
NIR	near infrared
O	oxygen delignification stage
OH	hydroxyl group
OH_{phen}	phenolic hydroxyl group
P	peroxide bleaching
PA	profiled alkalinity
Paa	peracetic acid stage
Q	chelating agent treatment stage
S	syringyl
S/N	signal to noise ratio
ThL	*Trametes hirsuta* laccase
TMP	thermomechanical pulp
UV	ultraviolet
UVRR	ultraviolet resonance Raman
UV-Vis	ultraviolet-visible
Z	ozone stage

Table of contents

1 Introduction

Today we are constantly looking for new renewable sources for different biomass products and particularly energy. Modern economical and effective processes for conversion of renewable biomass to fuels, other energy products such as electricity, as well as biomass based chemicals are developed. Wood biomass is an important renewable carbon source, which has potential uses not only in pulp and paper production but also as a raw material for bio-based chemicals, biofuels and bioenergy.

Lignin is nature's second most abundant polymer after cellulose (Fengel, Wegener 1984, Boerjan, Ralph et al. 2003). Hence, it is vastly available around the world in all woody plants. Simultaneously, lignin is a unique compound, since it is one of the most difficult natural polymers with regard to its structure and heterogeneity (Fengel, Wegener 1984). Many uncertainties still remain about the structure, formation, and reactions of lignin as well as its distribution in plant cells. The analysis of the lignin structure is challenging because of the complexity of the macromolecule itself, its limited solubility, and covalent bonding to carbohydrates inside the plant cell wall. The isolation of lignin from biomass introduces changes, regardless of the isolation method applied.

In order to be able to utilize lignin efficiently and sustainably, potent analytical techniques are needed. Only few wet-chemical and spectroscopic techniques are available to study the structure of lignin directly in wood or in pulps. Raman spectroscopy is a nondestructive technique that is applicable to study lignin *in situ*, even if the lignin content is very low.

Raman spectroscopy is a technique that detects vibrations in molecules based on Raman scattering (Smith, Dent 2005). It has become a widely used technique to gain information on chemical structures, as well as to identify and to determine the amount of substances in the sample (Gierlinger, Schwanninger 2007). In addition to its versatile applicability in academic research, Raman spectroscopy provides a fast and simple analysis method for a large series of samples in the industry, as there is no need for sample preparation with chemicals. Advances in Raman instrumentation and spectral processing have enabled the use of Raman spectroscopy also by non-specialists in laboratories and on-line chemical production plants around the world (Pelletier 1999, Pelletier 2003).

2 Background

2.1 Wood biomass

Wood biomass consists of different kinds of cells that provide mechanical support, water transport and metabolism to the living tree (Stenius 2000). A tree grows in height by forming new cells at the tip of its trunk and at the ends of its branches (Forss, Fremer 2003). Wood cells are chemically heterogeneous and consist of a polymeric matrix of cellulose, hemicelluloses and lignin (Stenius 2000, Fengel, Wegener 1984). A general scheme of the chemical wood components is presented in Figure 1.

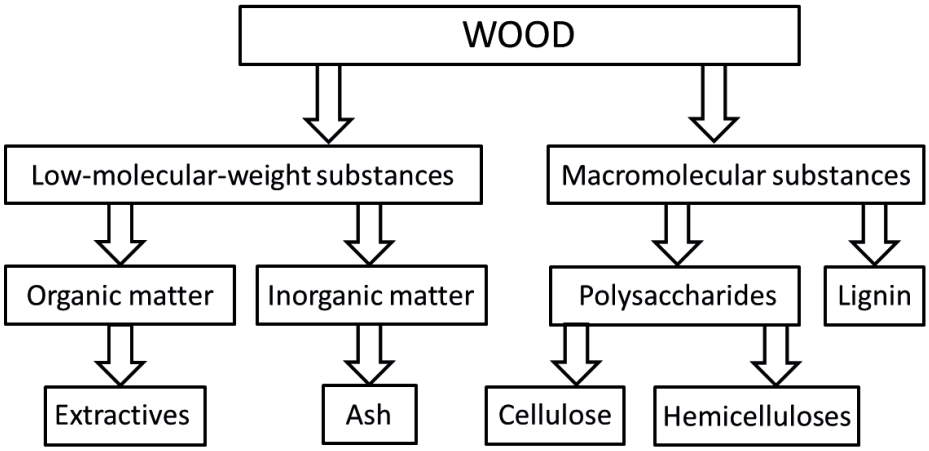

Figure 1. General scheme of the chemical wood components (Fengel, Wegener 1984).

Wood in most conifers is more than 90% composed of one type of cell, whereas the wood in deciduous trees is composed of several types of cells present in proportions that are characteristic of each species. Each cell produces its components according to its specific needs. Different types of cells may therefore produce different carbohydrates and lignins (Forss, Fremer 2003).

2.1.1 Cellulose

Cellulose is the major structural wood component, which constitutes approximately one half of both softwood and hardwoods. It is nature's most abundant polymer. Cellulose is a linear, high-molecular weight polymer built up of β-D-glucose (anhydroglucopyranose).

These glucose units of cellulose are linked to each other via 1-4-glycosidic linkages, and two of them form a cellobiose unit as the repeating unit of a cellulose polymer (Fengel, Wegener 1984).

According to the so-called fringed-fibrillar model of native cellulose, the polysaccharide chains are arranged into longitudinal threads called microfibrils where crystalline and amorphous domains appear after each other at irregular intervals (Mark 1940, Hearle 1963, Scallan 1971, Kontturi, Suchy et al. 2011).

In the chemical pulp production, the objective is to isolate cellulose and to remove all of the lignin in wood fibers without affecting the carbohydrates. This is performed by cooking and bleaching the pulp. Today cellulose is seen as a major potential source of glucose for the subsequent production of biofuels, especially in bioethanol production.

2.1.2 Hemicelluloses

Wood contains substantial amounts of other polysaccharides in addition to cellulose. Most of these polysaccharides, which in general not only have a much lower molecular mass but are also much easier to hydrolyze than cellulose, are jointly called hemicelluloses (Forss, Fremer 2003). Unlike cellulose, hemicelluloses are constructed of various monosaccharide units, thus becoming heteropolysaccharides. Hemicellulose chains are much shorter than cellulose chains, and hemicelluloses are often branched, with side-groups. The main types of hemicellulose monosaccharides are hexoses (glucose, mannose, galactose), pentoses (xylose and arabinose), deoxyhexoses and uronic acids (Fengel, Wegener 1984).

During the alkaline kraft pulping process, the 4-O-methylglucuronic acid groups from xylan can be converted into hexenuronic acid (HexA) groups. HexA contributes to the consumption of bleaching chemicals without the actual bleaching effect.

2.1.3 Lignin

Lignin is an amorphous polymer with a chemical structure that distinctly differs from the other macromolecular constituents of wood (Stenius 2000). It plays a key role in most of the reactions occurring in chemical wood pulping and bleaching, as well as in other processes in which wood is subjected to chemical treatments (Forss, Fremer 2003).

Lignin is a complex polymer linked via oxidative coupling that is probably catalyzed enzymatically by both peroxidases and laccases (Boudet, Lapierre et al. 1995). A proposed

structure for softwood lignin is shown in Figure 2. Lignin and other wood components are not separate chemical entities but integrated parts of an enormous molecular network that forms the cell walls and links cells together (Forss, Fremer 2003). In wood, lignin is bound to polysaccharides by covalent bonding (Fengel, Wegener 1984). The most prominent functional groups in lignin are the hydroxyl, methoxyl, carbonyl and carboxylic groups, which are attached to aliphatic chains or phenyl groups of the polymer.

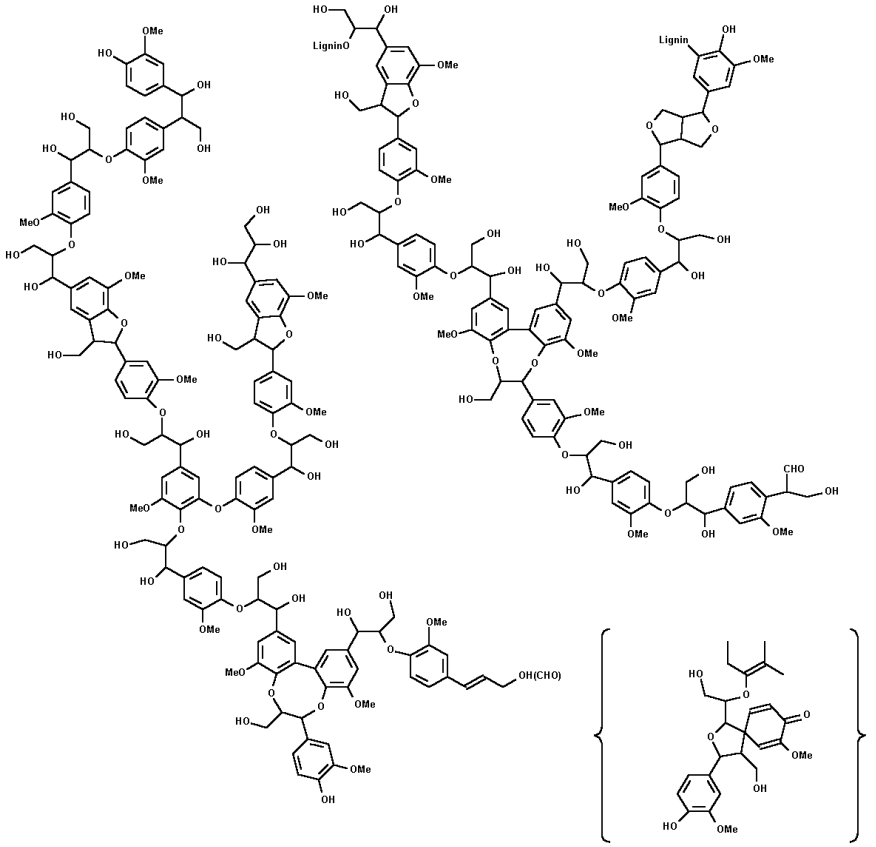

Figure 2. The softwood lignin structure as proposed by Brunow (Brunow 2001).

Lignin brings mechanical strength to tree stems and trunks, and hydrophobicity to their water-conducting vascular elements. According to the prevailing hypothesis, plant lignin is mainly constructed of aromatic phenylpropanoid units (*p*-hydroxycinnamyl alcohols). It is an amorphous heteropolymer consisting of three types of monomer units or precursors

that differ from each other based on the number of methoxyl groups attached to the aromatic ring. The most important building units of lignin are *para*-coumaryl, coniferyl and sinapyl alcohol monomers (Figure 3) (Stenius 2000).

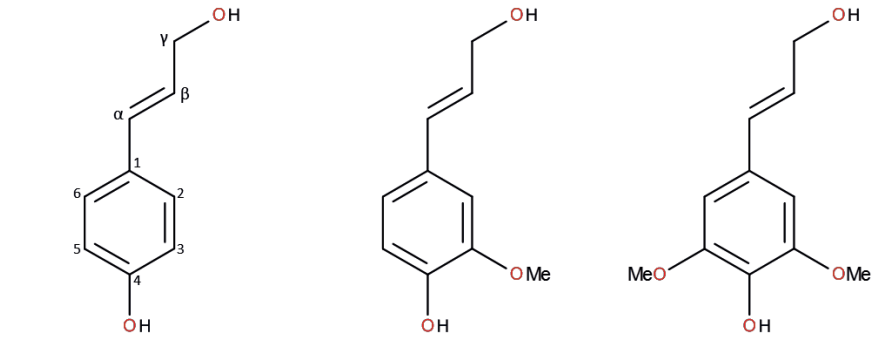

trans-p-Coumaryl alcohol *trans*-Coniferyl alcohol *trans*-Sinapyl alcohol

Figure 3. The three precursors of lignin.

These monomers produce *p*-hydroxyphenyl (H), guaiacyl (G) and syringyl (S) units respectively when included in the lignin polymer (Stenius 2000). Softwood lignin is mainly composed of coniferyl alcohol and, therefore, softwood lignin is referred to as guaiacyl lignin. Hardwood lignin is mainly composed of coniferyl and sinapyl alcohol, and it is referred to as guaiacyl-syringyl lignin. Lignin found in grasses is composed of all three types of precursors, thus being referred to as *p*-hydroxyphenyl-guaiacyl-syringyl lignin (Fengel, Wegener 1984).

The structural building units of lignin are joined together by ether linkages (C-O-C) and carbon-carbon bonds (C-C) (Stenius 2000). These linkages can be seen in Figure 2. The most prominent linkage type in wood is the β-O-4 structure (Stenius 2000, Boerjan, Ralph et al. 2003). The other common linkages found are β-5, β-β, 5-5, β-1, 5-O-4 and α-O-4 (Boerjan, Ralph et al. 2003). Also other structures, such as dibenzodioxocin, have been found in wood (Karhunen, Rummakko et al. 1995).

2.2 Wood-biomass processing

2.2.1 Pulping

Pulping refers to various processes where wood or other fibrous biomass is converted into a product with liberated fibers. Pulping can be performed via chemical or mechanical processes, and the term 'pulp' is collectively used for chemical, chemimechanical and mechanical pulps. In chemical pulping lignin (and hemicelluloses) are dissolved and removed from fibers, and in mechanical pulping fibers are mechanically softened by refining, with the help of elevated temperatures and/or pressure.

Thermomechanical pulping

In the production of thermomechanical pulp (TMP) the wood chips are preheated with pressurized steam and refined under pressure at elevated temperatures (140°C-155°C) (Sundholm 1999).

Kraft pulping

In conventional kraft (sulfate) pulping, sodium hydroxide (NaOH) and sodium sulfide (Na_2S) are used for chemically cooking the wood chips. Lignin and hemicelluloses degrade to generate fragments that are soluble in the strongly basic liquid (Stenius 2000).

Bleaching

Bleaching is a chemical process applied to mechanical and chemical pulps in order to increase their brightness. Bleaching is performed either by removing the residual lignin of chemical pulps of by converting and stabilizing chromophoric groups of mechanical pulps. Residual lignin removal is done in a bleaching sequence comprising a series of bleaching stages, usually with intermediate washing between the stages. Common bleaching chemicals today are oxygen, chlorine dioxide, hydrogen peroxide and ozone (Stenius 2000).

2.2.2 Enzymatic treatment

Enzymes are natural catalysts, and, as such, very efficient and specific. They generally catalyze only one type of reaction each, for example the oxidation of a substrate.

Laccases are oxidative enzymes suited for activation of lignin-containing fibers before functionalization. Laccases need molecular oxygen for oxidizing various aromatic and non-aromatic compounds by a radical reaction mechanism (Claus 2003, Claus 2004).

2.3 Traditional lignin characterization from wood-based biomass

More than a century of lignin research has produced findings that are largely quite unconnected with each other and also difficult to reproduce (Forss, Fremer 2003). Traditionally most analytical and spectroscopic techniques used to characterize lignocellulosic wood biomass require the separation and isolation of components. The isolation is usually the time-determining step in the analytical procedure (Saariaho, Hortling et al. 2003). The isolation yields are often low and impure, and these complicated procedures can disrupt the studied structures (Tamminen, Liitiä et al. 2004). Additionally, chemical pretreatments consume chemicals, and, therefore, increase the cost of the analysis.

The quantitative extraction of lignin from wood requires splitting of the lignin-carbohydrate bonds and transforming lignin into soluble derivatives, i.e. lignin preparations (Forss, Fremer 2003). Thus the structure of lignin is altered in the process. This can hinder the analysis of different linkages and functional groups in lignin, and alter its molar mass. For a low lignin content, for example in bleached pulps, the accuracy of the most commonly applied residual lignin determination methods (such as Klason lignin content) is relatively poor (Jääskeläinen, Saariaho et al. 2005). Hexenuronic acids (HexA) are also tedious to determine using conventional analytical methods as they are very sensitive to degradation in acidic environment (Stenius 2000).

However, the traditional wet-chemical methods are of great importance even today, although they have been replaced, to some extent, by less tedious and time-consuming instrumental techniques.

2.4 Modern lignin characterization techniques from wood-based biomass

Techniques which can be used to analyze lignin and other wood components without the isolation step include, e.g., analytical pyrolysis, nuclear magnetic resonance (NMR) spectroscopy, X-ray photoelectron spectroscopy (XPS/ESCA), ultraviolet and visible light (UV-Vis) spectroscopy, Fourier transform infrared (FTIR) spectroscopy, fluorescence spectroscopy and Raman spectroscopy.

Pyrolysis-gas chromatography/mass spectrometry (Py-GC/MS) is rapid and sensitive technique for characterizing the chemical structure of lignin, which allows the analysis of very small amounts of sample without prior manipulation and/or isolation (del Río, Gutiérrez et al. 2005, Lin, Dence 1992).

NMR spectroscopy is based upon the absorption of radio waves by certain nuclei in organic molecules when they are in a strong magnetic field (Fessenden, Fessenden 1994). NMR has a high resolution, enabling a larger amount of information to be obtained in lignin analysis. Quite often, ^{13}C NMR is used for the estimation of some specific moieties (Capanema, Balakshin et al. 2004). Two-dimensional NMR spectroscopy has been used to characterize for example lignin-carbohydrate complex linkages (Balakshin, Capanema et al. 2011).

XPS is a tool for determining surface coverage by lignin, extractives and carbohydrates. When the monochromatic X-rays kick off electrons from core orbitals, only the surface region electrons are emitted and analyzed (Johansson, Campbell et al. 1999, Orblin, Fardim 2010).

In pulp research, UV-Vis reflectance spectroscopy has traditionally been used to investigate the formation of pulp chromophores during ageing, as has been described in the review by Schmidt and Heitner (Schmidt, Heitner 1999). This method has also been shown to have a great potential ability to monitor other colorless UV-active components of kraft pulp during bleaching (Ragnar 2001, Liitiä, Tamminen et al. 2004). Changes induced by bleaching in the structures of lignin, hexenuronic acid (HexA), and carbonyl contents of pulps can be studied using UV-Vis reflectance spectroscopy (Ragnar 2001, Liitiä, Tamminen et al. 2004). By converting reflectance spectra to absorbance (k/s) spectra using the Kubelka-Munk equation, it is possible to follow the changes in the content of these UV-active pulp components (Liitiä, Tamminen et al. 2004).

Absorption of ultraviolet or visible radiation results in electronic transitions, promotion of electrons from low-energy ground-state orbitals to higher-energy excited-state orbitals (Fessenden, Fessenden 1994). Colored compounds absorb light in the visible region, and they have more easily promoted electrons than compounds that absorb at shorter UV wavelengths (Fessenden, Fessenden 1994). The absorbance at the excitation wavelength is proportional to the fluorescence emission intensity. On absorbing radiation one electron is excited to a higher energy state. Fluorescence emissions occur when first excited singlets relax to ground states (Brown 1980).

In fluorescence spectroscopy the fluorescence emission from a sample is analyzed. The electrons in a sample are excited by incident light, and the emitted light from the sample is then detected. Fluorescence spectroscopy is currently a widely used methodology used, especially in biotechnology area (Lakowicz, Masters 2008).

In FTIR spectroscopy a sample is irradiated with infrared (IR) light. The sample absorbs part of the radiation, and the light that goes through the sample is collected at a detector. A Fourier transform is required to turn the raw data into the actual spectrum. Infrared spectroscopy has a variety of uses in the chemical analysis, including competitive analysis, quantification of individual components, and identification of contaminants in the sample (Conners 1995).

Raman spectroscopy is an analytical technique based on Raman scattering. A typical measurement time for a single spectrum with visible or ultraviolet laser excitation is 10 to 30 seconds in total, depending on the sample. The most common choice for excitation in Raman spectroscopy is a visible laser. Ultraviolet resonance Raman (UVRR) spectroscopy is also a very effective method for studying even the trace amounts of aromatic and other unsaturated compounds, since the resonance effect enhances Raman signals from these compounds. As the powerful UV laser light can cause degradation in biomass-based samples, the samples have to be spun on a sample table during the measurement. This allows for a single spot of the sample to not be radiated with UV light for a long time during the spectral collection. However, this spinning results in a random fiber orientation with respect to the laser light polarization.

2.5 Raman spectroscopy in wood chemistry

Raman spectroscopy was first utilized on wood biomass studies in the 1980's (Atalla, Agarwal 1985, Agarwal, Atalla 1986). The development of Raman spectroscopic techniques, including the development of lasers, monochromators, and sensitive detectors, has made it a fascinating analytical tool in wood chemistry (Conners 1995). Raman spectroscopy is a powerful method for structural analysis of lignin (Saariaho, Jääskeläinen et al. 2004, Jääskeläinen, Saariaho et al. 2005, Agarwal, Ralph 2008, Pandey, Vuorinen 2008). The modification or isolation of lignin is not necessary, and various forms of sample are suitable for direct analysis of lignin in a mixture with other materials, in solutions, slurries, emulsions, powders, fibers, pellets and films (Sjöström, Alen 1999, Pelletier 2003, Larsen, Barsberg 2010).

In lignin studies, Raman spectroscopy provides structural information on lignocellulosic materials *in situ* (Lin, Dence 1992, Agarwal 1999, Glasser, Northey et al. 2000, Barsberg, Matousek et al. 2005, Saariaho, Jääskeläinen et al. 2003, Saariaho, Argyropoulos et al. 2005, Lähdetie, Liitiä et al. 2009, Lähdetie, Liitiä et al. 2009, Zakzeski, Bruijnincx et al. 2011, Saariaho, Hortling et al. 2003). Raman spectra can be obtained directly from single

plant cells or pulp fibers, and a specified area can be imaged (Schulz, Baranska 2007). The applications on plants range from investigations on structural polymers to metabolites and mineral substances, while chemical and structural information can be obtained directly in the native state (Gierlinger, Schwanninger 2007). Raman spectroscopy is insensitive to the polar bonds in a water molecule, which is an advantage in the analysis of water-containing wood biomass samples.

The Raman signal of lignocellulosic fibers is sensitive to the orientation of the fibers when using a polarized light in analysis (Wiley, Atalla 1987).

The major limitation of the application today is the simultaneously emitted laser-induced fluorescence (LIF), which makes the analysis difficult or even impossible using the traditional Raman spectroscopy with visible light excitation (Conners 1995, Agarwal 1999). LIF background originates mainly from lignin structures, and it overlaps with Raman bands. This background signal can in the worst case overwhelm the weaker Raman signal completely. Hence, LIF obstructs the sample characterization, and restricts the use of Raman spectroscopy when the excitation energy falls in the visible range. To avoid the problem of fluorescence with lignocellulosic samples, near infrared (NIR) Raman excitation wavelength can be used since NIR excitation is too low in energy to emit fluorescence. Fluorescence rejection systems can also be used to avoid fluorescence (Agarwal 1999, Agarwal, Terashima 2003, Barsberg, Matousek et al. 2006, Nuopponen 2005, Saariaho, Jääskeläinen et al. 2004). While for Raman imaging whole plant organs, such as seeds, fruits, and leaves, the lateral resolution with the NIR-FT Raman technique is adequate, the study of the lower hierarchical level of cells and cell walls need high resolution gained with a visible laser based system (Gierlinger, Schwanninger 2007). Fluorescence in the visible range hinders also the analysis of moieties that absorb visible light, such as chromophoric lignin structures.

Alternatively, by using ultraviolet (UV) excitation the fluorescence emission is shifted to a higher spectral range, and hence it does not overlap with the Raman signal. Consequently, UV resonance Raman offers an effective way to overcome the fluorescence problem in wood biomass research (Saariaho, Hortling et al. 2003, Smith, Dent 2005).

The utilization of UV light in excitation not only resolves the problem of fluorescence but additionally enhances the signals arising from aromatic lignin and other unsaturated structures. UV resonance Raman spectroscopy has been successfully used in the analysis of hexenuronic acid (HexA) groups in pulps (Halttunen, Vyörykkä et al. 2001, Saariaho, Jääskeläinen et al. 2003, Jääskeläinen, Saariaho et al. 2005). Lignin is typically detected at

ca. 280 nm (Halttunen, Vyörykkä et al. 2001), while hexenuronic acid absorption maximum is detected at ca. 230 nm (Teleman, Harjunpää et al. 1995). Thus UV excitation produces enhanced Raman spectra for these compounds. The main Raman band of lignin is detected at ca. 1600 cm^{-1}. In HexA the conjugated C=C double bond structure gives rise to the shoulder at ca. 1657 cm^{-1} in the kraft pulp spectrum (Halttunen, Vyörykkä et al. 2001, Saariaho, Hortling et al. 2003). Using UV excitation in Raman spectroscopy enables the characterization of even trace amounts of lignin, for example, in fully-bleached pulps *in situ*.

2.6 Basic theory of Raman spectroscopy

Light is made up of photons, which are elementary particles carrying the electromagnetic force. When matter is irradiated with light, the photons may be absorbed or scattered, or they may pass straight through it (Smith, Dent 2005). If the energy of a photon corresponds to the energy gap between the ground state and an excited state of a molecule, the photon may be absorbed and the molecule is promoted to an excited state (Smith, Dent 2005). However, the photon can also interact with the molecule even though the energy of the photon does not match the difference between the two energy levels of the molecule (Smith, Dent 2005). In this case, the photon is scattered from the molecule after interacting with it.

If the scattering is elastic, and the molecule is relaxed back to its original ground state (m) after interacting with the photon, the phenomenon is called Rayleigh scattering (Figure 4) (Smith, Dent 2005). It occurs when the electron cloud relaxes without any nuclear movement. This process is intense, and generally the Rayleigh scattering is the dominant process (Smith, Dent 2005).

If the light and the electrons interact and also the nuclei begin to move at the same time, Raman scattering occurs (Smith, Dent 2005). In Raman scattering the energy can be transferred either from the incident photon to the molecule or from the molecule to the scattered photon. Raman scattering is inelastic, and the energy of the scattered photon is different from that of the incident photon by one vibrational unit (Smith, Dent 2005). If the process starts with a molecule in the ground state (m) which is then excited to a higher energy vibrational state (n), the process is called Stokes scattering (Smith, Dent 2005). If the molecule is originally in a vibrationally excited state (n) due to thermal energy, and it then relaxes to the ground state (m), the process is called anti-Stokes scattering. Thus anti-Stokes scattering involves a transfer of energy to the scattered photon from the molecule

(Smith, Dent 2005). Either way, Raman scattering is a very weak process, as from all scattered photons only one in every 10^6-10^8 photons are Raman scattered (Smith, Dent 2005) . The different types of scattering are presented in Figure 4.

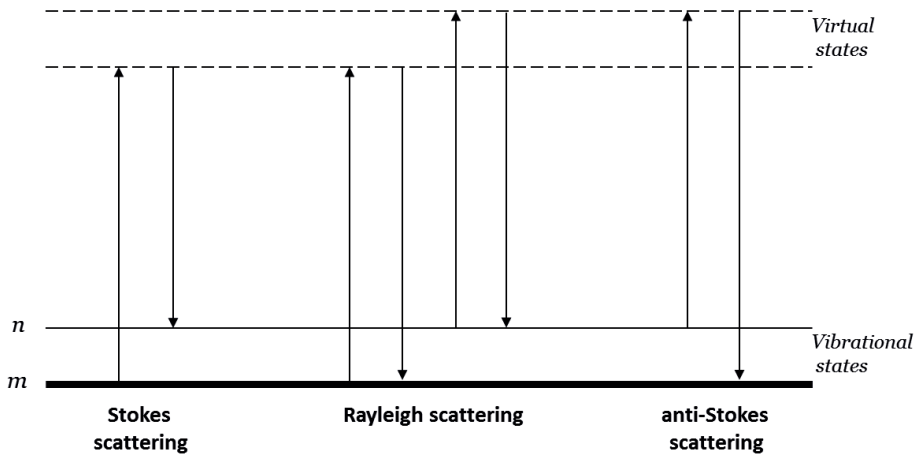

Figure 4. Diagram of the Raman and Rayleigh scattering processes.

Usually Raman scattering is recorded only as Stokes scattering. Sometimes anti-Stokes scattering is preferred if, for instance, fluorescence interference needs to be avoided, as fluorescence requires absorption of energy from the photons to the irradiated molecules (Smith, Dent 2005).

Intense Raman scattering is produced from vibrations which change the polarizability of the electron cloud in a chemical bond during an inelastic collision with incident light (McCreery 2000). The most intense Raman scattering originates from nonpolar bonds having symmetrical charge distributions and thus symmetric vibrations (McCreery 2000). Large polarizability changes occur with vibrations involving polarizable atoms, typically a second- or third-row element such as S, Cl, Br or I. With the first-row elements C, N and O of which most of the biologically important molecules are largely constructed, the atomic polarizability is small (Brown 1980). Nevertheless, high Raman intensities can result from systems involving double bonds or delocalized electrons, in particular aromatic compounds (Brown 1980).

This is in contrast to infrared (IR) absorption (often called Fourier transform infrared (FTIR) absorption), as the IR spectroscopy detects mostly polar bonds, although it

operates at the same energy range as Raman spectroscopy (Figure 5) (McCreery 2000). The intensity of IR absorption is proportional to the amount by which the dipole moment of the molecule changes during the vibration (Brown 1980). Even though IR and Raman spectroscopies completely differ experimentally, a molecular vibration may give rise to features in either or both of them (Brown 1980). Thus these two spectroscopic techniques can produce quite different intensity patterns, and they are complementary methods for detecting the vibrational structure of a molecule (Smith, Dent 2005) .

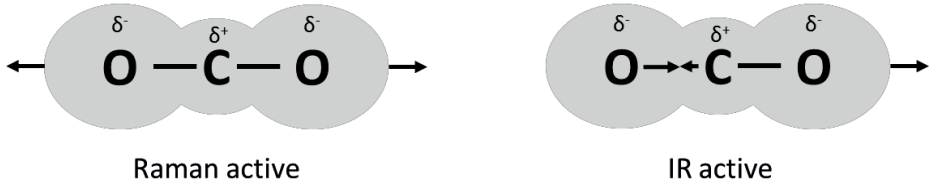

Figure 5. Electron cloud model of carbon dioxide showing Raman and IR active vibrations (Smith, Dent 2005).

The intensity (I) of the Raman scattering is related to the power (l) of the laser used in excitation, the square of the polarizability (α) of the molecule analyzed, and the fourth power of the frequency (ω) of the exciting laser, as defined by simplified Equation [1] (Smith, Dent 2005). Parameter K consists of constants, such as the speed of light.

$$I = Kl\alpha^2\omega^4 \qquad [1]$$

Therefore, the intensity of the Raman scattering can be controlled by adjusting the power of the laser, and the frequency (i.e. the wavelength) of the incident laser light. The molecular polarizability remains as the property of the analyzed matter.

2.6.1 Resonance enhancement

To obtain resonance Raman scattering, a laser beam with an excitation frequency close to that of an electronic transition of the molecule is chosen (Smith, Dent 2005). The wavelength of the incident light is equal or close to the absorption wavelength. The molecule is then excited to the higher electronic state (Figure 6).

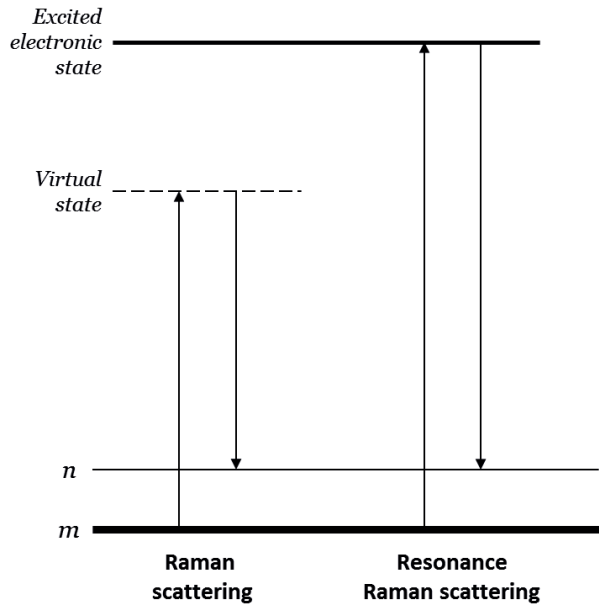

Figure 6. Spectroscopic transitions of Raman and resonance Raman scattering.

This results in enhanced Raman signals of the order of ca. 10^2-10^6 (Smith, Dent 2005). The key difference between absorption and resonance Raman scattering is the length of time the molecule remains in an excited state (Smith, Dent 2005). The Raman scattering process is fast, but the absorption process is slower as the electron is absorbed into the molecule (Smith, Dent 2005).

Simply put, the resonance enhancement means that vibrations from the resonant groups can be selectively identified (Smith, Dent 2005). When the resonant condition occurs, it is possible to analyze the resonant molecules also in trace amounts, if the matrix does not greatly contribute to the spectrum. Thus, it is possible to obtain high sensitivity for selected structures by tuning the wavelength appropriately. In addition to vibrational information also electronic information can be obtained, and resonance Raman spectroscopy has long been used for studying organic materials (Brahma, Hargraves et al. 1983).

As said, with a suitable frequency for resonance enhancement not only resonance Raman scattering but also absorption will occur (Smith, Dent 2005). As absorption occurs, the energy may be lost either by transfer to the lattice, and dissipation as heat or as fluorescence (Smith, Dent 2005). How much radiation will be absorbed is determined by the properties of the molecules. Fluorescence can limit the number of molecules which will

be suitable for resonance Raman spectroscopic studies (Smith, Dent 2005). However, fluorescence is not a problem in ultraviolet resonance Raman (UVRR) spectroscopy, as explained in Section 2.6.3.

2.6.2 Fluorescence in Raman spectroscopy

Fluorescence phenomenon is the emission of light by molecules that have absorbed incident light. Fluorescence is generated when a molecule relaxes from one electronic state to another of lower energy (Brown 1980). The emitted light has longer wavelength, and therefore lower energy, than the absorbed radiation (Fessenden, Fessenden 1994). Fluorescence involves two interactions and two photons, i.e. absorption and subsequent emission (Brown 1980). Each process is practically instantaneous, but there is a time lag between them during which the molecule exists in an electronically excited state (Brown 1980).

The main disadvantage of using Raman spectroscopy is fluorescence. Fluorescence is induced by the exciting laser light, and it is a notably larger problem in the visible region than in the ultraviolet (UV) or the near-infrared (NIR) regions. When molecules are irradiated with a laser beam, Raman signal is instantaneously emitted. Fluorescence is a slower phenomenon, and it is emitted on a substantially longer time-scale, typically in nanoseconds (Figure 7) (Matousek, Towrie et al. 1999, Matousek, Towrie et al. 2001, Lakowicz, Masters 2008).

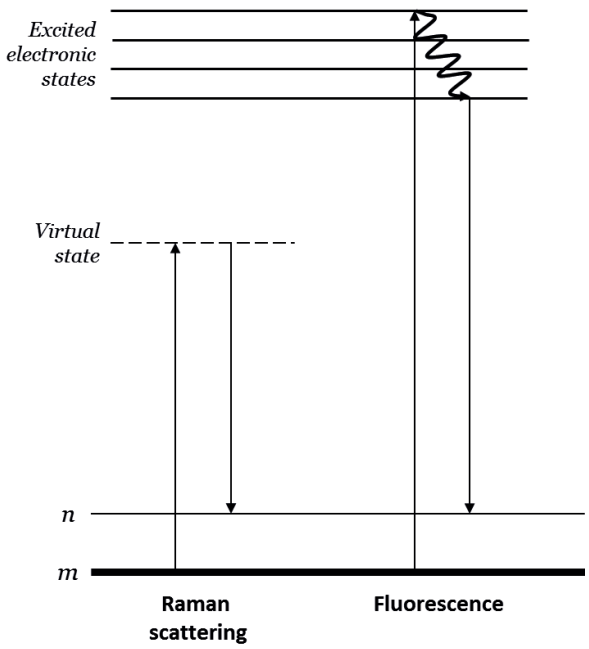

Figure 7. Spectroscopic transitions of Raman scattering and fluorescence.

Fluorescence background can overlap with Raman bands, and it can, in the worst case, overwhelm the weaker Raman signal completely. Hence, fluorescence obstructs the sample characterization, and restricts the use of Raman spectroscopy when the excitation energy falls in the visible range. To avoid the problem of fluorescence, NIR Raman excitation can be used since NIR excitation is usually too low in energy to emit fluorescence. Alternatively, UV excitation shifts the fluorescence emission to a higher spectral range and, therefore, it does not overlap with the Raman signal. Consequently, the fluorescence-free spectra can be obtained. Fluorescence rejection systems, such as Kerr gate, do exist, but they are under development (Agarwal 1999, Agarwal, Terashima 2003, Barsberg, Matousek et al. 2006, Nuopponen 2005, Saariaho, Jääskeläinen et al. 2004). Fluorescence in the visible range furthermore hinders the analysis of moieties, such as chromophoric structures, that absorb visible light. In fact, fluorescence is currently the most important factor that limits the applicability of Raman spectroscopy not only in the biomass sample characterization but in several other applications as well.

2.6.3 Ultraviolet excitation

The fourth power nature of the scattering (Eq. 1) makes high frequency ultraviolet (UV) Raman scattering remarkably more sensitive than visible Raman scattering (Smith, Dent 2005). Many compounds, such as lignin, also absorb UV radiation, the resonance of which enhances the Raman signal, thus making the UV Raman scattering even more sensitive towards absorbing structures.

Fluorescence is no longer a problem at this very short wavelength (Smith, Dent 2005). Most systems contain enough vibronic states for the energy to be dissipated into the material, and, even if it is emitted, the emission is well outside the region used for Raman detection (Smith, Dent 2005). This is because the energy difference between the excitation and fluorescence emission (ΔE_F) is much larger than the difference between the excitation and Raman-scattered light (ΔE_R) (Figure 8). This causes the fluorescence to occur at much higher wavenumbers than those corresponding to the vibrational energy levels observed in Raman spectroscopy.

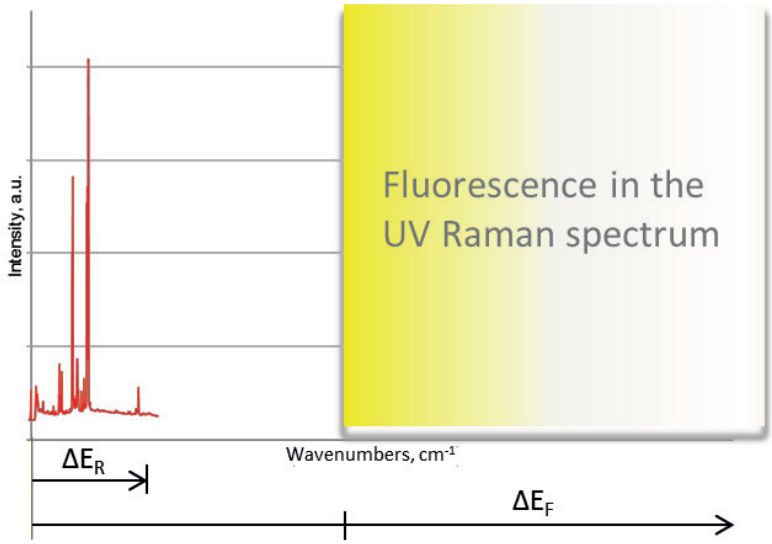

Figure 8. Fluorescence in the UV Raman spectrum.

However, the drawback in UV excitation is the high energy radiation that can cause degradation of the samples. This degradation can also obstruct the UV Raman imaging or mapping of organic samples. Therefore the samples are usually spun on the sample table and the measurement time is kept short in order to reduce the problem of burning.

2.6.4 Development of Raman spectroscopy in chemical analysis

The Raman effect was observed experimentally for the first time in 1928 by Raman and Krishnan (Raman, Krishnan 1928). The major impediment in using Raman spectroscopy was the weakness of the Raman effect itself (McCreery 2000). Furthermore, the problem of fluorescence with visible light excitation inhibited the use of the technique for decades, as well as inefficient light collection and detection techniques. Raman spectroscopy was not applied much in chemical analysis before 1980's (Brown 1980, McCreery 2000). Since the development of lasers, Fourier Transform (FT) Raman technique, edge and notch filters, multichannel detectors and charge-coupled devices, Raman spectroscopy has been used increasingly in practical applications (McCreery 2000).

The development of Raman instruments has quite recently enabled easy Raman imaging and mapping (Zoubir 2012). There are different imaging methods available, such as point mapping, line scanning and global imaging (Zoubir 2012).

3 Objectives of this work

The objective of this research was to study and broaden the applicability of Raman spectroscopy in wood biomass research, especially in the analysis of the structure and reactions of lignin.

In order to obtain a more detailed understanding of bleaching chemistry and applicability of Raman spectroscopy in bleaching studies, unbleached and bleached kraft pulps were analyzed using Raman and reflectance UV-Vis spectroscopy in **Paper I**. To gain information on the chemical changes in thermomechanical pulp (TMP) during enzymatic treatment, the TMP activation process with laccases was followed using spectroscopic analyses, namely Raman, UV-Vis and FTIR spectroscopy in **Paper II**.

To develop the quantitative Raman spectroscopic analysis method for phenolic hydroxyl group determination, the effect of pH on lignin analysis was investigated using lignin model compounds and wood pulps in **Paper III**. Lignin model compounds were used to effectively represent different linkages and functional groups in the otherwise very complex lignin polymer. Different lignin model compounds were also used in **Paper IV** to study laser-induced fluorescence (LIF) of lignin in Raman spectroscopy. LIF is the most important factor hindering the use of Raman spectroscopy with wood-based samples, especially at visible excitation. Fluorescence and UV-Vis absorbance spectroscopic techniques were used as well to further investigate the fluorescence properties of the studied lignin model compounds. In addition, wood and pulp samples were analyzed and compared to different polymeric lignins in order to determine how well these lignin polymers represented the structure of native lignin in wood.

In **Paper V** the effect of excitation wavelength on the Raman spectra of wood-based samples was investigated. In this study several different lasers were used to obtain excitation ranging from ultraviolet (UV) to near infrared (NIR) radiation to see how the different laser frequencies affected the Raman spectra of pulp and wood samples.

4 Materials and methods

4.1 Materials

4.1.1 Wood and Pulps

Spruce chips (*Picea abies*) and eucalyptus chips (*Eucalyptus globulus*) were investigated.

The pulp samples studied in this work were mechanical pulps, kraft pulps, semi-bleached pulps, and fully-bleached pulps processed from softwoods and hardwoods.

4.1.2 Enzymes

In this work two different laccase enzymes, namely *Trametes hirsuta* (ThL) and *Melanocarpus albomyces* (MaL), were used for functionalizing spruce thermomechanical pulp (TMP).

4.1.3 Model compounds

Lignin model compounds were used in this work to study the reactions and structure of lignin, as they represent different linkages and functional groups in the complex lignin polymer. Also different polymeric lignins were studied in order to find out how well the lignin polymers represent the structure of native lignin.

Phenolic model compounds of lignin, namely phenol, guaiacol, syringol, *p*-cresol, 2-MeO-*p*-cresol, 4-Me-syringol and iso-eugenol were used for observing the effect of pH on UV resonance Raman spectra.

Lignin model compounds erol, bierol, dibenzodioxocin as well as lignin polymers milled wood lignin (MWL), enzyme acidolysis lignin, and dehydrogenation polymer (DHP) lignin were used to investigate the laser-induced fluorescence of lignin in Raman spectroscopy.

4.2 Methods

4.2.1 Raman spectroscopy

UV resonance Raman (UVRR) spectroscopy

UVRR spectra in **Papers I**, **II**, **III** and **V** with the excitation wavelengths 229, 244 and 257 nm were collected with a Renishaw 1000 UV Raman spectrometer equipped with a Leica DMLM microscope and an Innova 90C FreD frequency-doubled Arq ion laser (Coherent, Inc., Santa Clara, CA, USA). The output power of the laser was adjusted to 10 mW, and the laser beam was attenuated with a neutral density filter with 50% transmittance. After that, the beam was reflected by mirrors to a dielectric edge filter. The beam was further directed to the microscope equipped with a deep UV LMU-40X objective. Due to losses in the light path, the final power at the sample level was approximately 2 mW. The backscattered Raman light was passed through the microscope to the edge filters and was further focused on a 30 mm slit by an additional lens. The transmitted Raman beam was reflected by prism mirrors to a diffraction grating of 3600 grooves/mm and finally to the UV-coated, deep-depletion charge-coupled device camera. The spectral range was 500–2000 cm^{-1}, and the resolution was approximately 6 cm^{-1}. All spectra were baseline-corrected, and the band heights were normalized either to the cellulose band at 1095 cm^{-1} or to the highest aromatic band at approximately 1605 cm^{-1} (=1 a.u.).

Confocal Raman spectroscopy

In **Papers IV** and **V** the samples were analyzed using a confocal Raman spectrometer (WITec alpha 300R, WITec GmbH, Ulm, Germany). Raman spectra were measured using a frequency doubled Nd:YAG green laser (wavelength 532.14 nm, power ~30 mW) and a Nikon 20X (numerical aperture N.A.=0.50) air objective. The grating of the spectrometer used was 600 grooves/mm and the optical fiber used in collecting the scattered photons had a diameter of 50 μm. The excitation light was polarized horizontally in x-direction. For detection a sensitive electron multiplying (EM) CDD camera (Andor Newton DU970-BV, Andor Technology plc, Belfast, UK) was used.

Other Raman spectroscopy

In **Paper V** also other Raman instruments were used in order to utilize as many excitation wavelengths as possible within the UV-NIR range. The Raman spectrometers had excitation wavelengths of 325, 442, 514, 633 and 785 nm.

Equipment

325 nm and 442 nm:

HORIBA Jobin Yvon LabRam HR 800 micro-Raman spectrometer. 40X NUV (0.5 N.A.) objective. Diffraction grating 1800 grooves/mm. Notch/edge filters. The spectral range was 500–2000 cm^{-1} for 325 nm, and 800-1840 cm^{-1} for 442 nm.

514 nm and 633 nm:

HORIBA Jobin Yvon LabRam 300 micro-Raman spectrometer. Laser 633 nm with power 20 mW, and laser 514 nm with power 1.24 mW. 50X air objective (0.5 N.A.). Diffraction grating 1800 grooves/mm. Hole 1000 μm, slit 100 μm, no filters. The spectral range was 500–2000 cm^{-1}.

785 nm:

HORIBA Jobin Yvon HR800 UV. 50X air objective (0.5 N.A.) Diffraction grating 600 grooves/mm. Hole 300 μm, no filters. The spectral range was 500–2000 cm^{-1}.

4.2.2 Other spectroscopic methods

UV-Vis spectroscopy

In **Papers I** and **II** the UV-Vis reflectance spectra were recorded from different pulp handsheets by using a Perkin Elmer Lambda 900 spectrometer (Perkin Elmer, Boston) equipped with an integrating sphere. The measurements took place at 50% relative humidity. The wavelength range was 200-800 nm. The spectral data was processed with a UV WinLab software. The reflectance values were recorded against black (Ro) and white (Rwb) backings, and the infinite reflectance (R∞) was calculated from these spectra according to Equation [2] (Schmidt, Heitner 1999, Liitiä, Tamminen et al. 2004), where Rw is the reflectance of the white backing.

$$R_\infty + \frac{1}{R_\infty} = \frac{R_0 - R_{wb} + R_w}{R_w R_0} + R_{wt} \qquad [2]$$

The infinite reflectance spectra were converted into k/s curves using the Kubelka-Munk equation [3] (Schmidt, Heitner 1999, Liitiä, Tamminen et al. 2004).

$$\frac{k}{s} = \frac{(1 - R_\infty)^2}{2R_\infty} \qquad [3]$$

The UV-Vis absorbance spectra in **Paper IV** were recorded using Shimadzu UV-2550 UV-VIS Spectrophotometer. Model compound solutions were diluted with distilled water to ca. 0.03 mM concentration.

Fourier transform infrared (FTIR) spectroscopy

The FTIR spectra in **Paper II** were recorded using Bio-Rad FTS 6000 research grade FTIR spectrometer (Bio-Rad, Digilab, MA, USA) fitted with a photoacoustic cell (PAS) (MTEC 300). The spectra were baseline-corrected, and the band heights were normalized to the cellulose band at 1064 cm^{-1} (1 a.u.).

Fluorescence spectroscopy

Fluorescence spectra in **Paper IV** were recorded using a Perkin Elmer Luminescence spectrometer LS 50 B, and the spectra were processed using an FL Winlab software.

5 Results and discussion

The experimental work presented in this thesis discusses the use of Raman spectroscopy in wood biomass characterization. Only the main findings of the experimental work related to this thesis are summarized and discussed. A full description of all the results can be found in the attached **Papers I-V**.

5.1 Characterization of kraft pulps

Despite the extensive research work conducted on pulp bleaching over the decades, the chemistry of bleaching is far from being understood in details. This is mainly due to the lack of appropriate techniques to study the trace amounts of lignin present in the semi-bleached pulp. In chemical pulp bleaching, lignin is almost completely removed from wood fibers. However, the low concentration of lignin in the samples (0.1-4%) has made its analysis practically impossible using the traditional analytical techniques. UV resonance Raman (UVRR) spectroscopy is a nondestructive technique that is applicable to study trace concentrations of lignin *in situ*.

The examined samples were softwood kraft pulps cooked to different kappa levels under various conditions. One of the pulps was also bleached with varying chemical charges of chlorine dioxide, ozone, and peroxide, as well as with different elemental chlorine-free and totally chlorine-free sequences. The pulps were analyzed by both UVRR and reflectance UV-Vis spectroscopic methods to get a detailed understanding of bleaching chemistry, and applicability of Raman spectroscopy for bleachability studies. In addition, the two spectroscopic techniques were compared in order to figure out more detailed information on the sample structure. Combining these spectroscopic methods provided a unique starting point to identify the reactions occurring in pulp bleaching.

5.1.1 Unbleached Kraft pulps

The residual lignin structures of eight different softwood (SW) kraft pulps were studied with UV resonance Raman and UV-Vis spectroscopies. Four kraft pulps were cooked using the conventional kraft pulping method to kappa numbers 22.2-51.7. In addition, two profiled alkali (PA) cooked pulps (kappa numbers 34.6 and 17.3), one low-sulfidity (LS) pulp (kappa number 27.4) and one profiled alkali cooked pulp after oxygen delignification (kappa number 18.0), were studied to observe the changes which alter the pulping conditions and the extent of delignification induced in the residual lignin structure and

HexA content. The lignin and HexA contents of the pulps determined by traditional methods are provided in Table 1.

Table 1. Kappa numbers, hexenuronic acid group and lignin contents of unbleached softwood kraft pulps (**Paper I**).

Sample	Sample code	Kappa number (κ)	Hexenuronic acid (mmol/kg)	Lignin kappa*)
Softwood kraft pulp	SW-22	22.2	28.2	19.8
Softwood kraft pulp	SW-28	27.9	31.3	25.2
Softwood kraft pulp	SW-33	33.2	32.9	30.4
Softwood kraft pulp	SW-52	51.7	35.2	48.7
Low sulfidity pulp	LS-30	27.4	15	26.1
Profiled alkalinity kraft pulp	PA-30	34.6	42	31
Profiled alkalinity kraft pulp	PA-18	17.3	24	15.3
Profiled alkalinity kraft pulp, oxygen delignified	PA-O	18.0	40	14.6

*) The lignin kappa number was calculated as the difference between the standard kappa number and the kappa number from HexA.

The UVRR spectra of the softwood kraft pulps with different delignification degrees are shown in Figure 9. Because the absolute intensity of the spectra depended on the excitation light focus on the sample and the roughness of the sample, the spectra could not be compared without spectral processing. In this case, the carbohydrate (cellulose) content of these samples was presumed to remain nearly constant and, therefore, the UVRR spectra were normalized to the cellulose's glycosidic C-O-C stretching band at ca. 1098 cm^{-1}. In this way, the comparison of the UVRR spectra of different samples was straightforward, as the height of the bands was directly proportional to the concentration of corresponding structures in the samples.

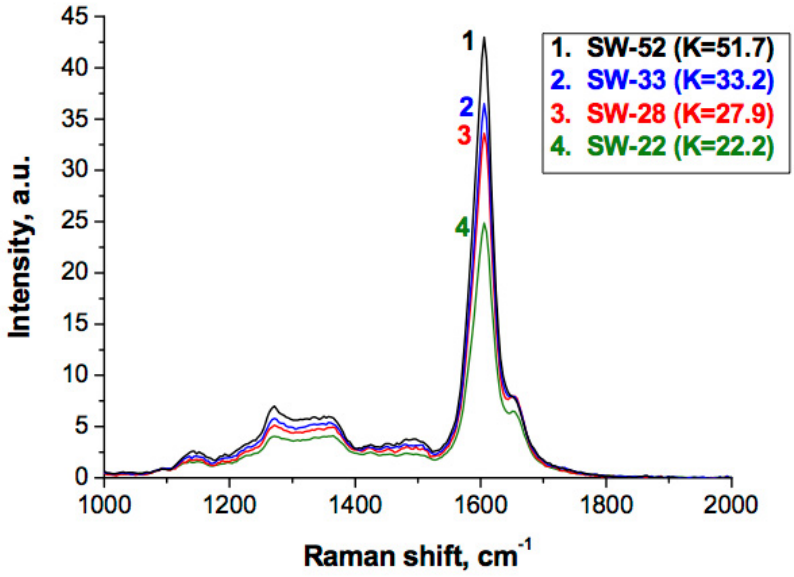

Figure 9. UVRR spectra of unbleached softwood (SW) kraft pulps with kappa numbers ca. 22-52. The heights of the spectra were normalized to the cellulose band at 1098 cm^{-1} (**Paper I**).

The UVRR spectra of unbleached softwood kraft pulps show the aromatic stretching band clearly at ca. 1605 cm^{-1}. The height of this band correlated directly with the lignin kappa number of these pulps; the higher the kappa number, the higher the aromatic stretching band. Similar correlation has also been observed earlier (Saariaho, Hortling et al. 2003, Jääskeläinen, Saariaho et al. 2005).

The shoulder at ca. 1658 cm^{-1} arises from the unsaturated and carbonyl structures in the samples (Halttunen, Vyörykkä et al. 2001). The intensity of this band was clearly the lowest for the pulp cooked to kappa 22.2, while it was nearly constant for the other conventionally cooked kraft pulps. For these pulps, the main origin of this band is hexenuronic acid, although other structures, such as ethylenic and carbonyl structures in lignin or extractives, may contribute to this band. Based on chemical analyses, the hexenuronic acid group content of these pulps decreased by ca. 25% during further cooking to kappa 22.2 (Table 1), which explains most of the decrease in this C=C stretching band.

The UV-Vis spectra (k/s) of unbleached softwood kraft pulps in Figure 10 show distinct changes during pulping. The height of the aromatic absorption band at ca. 280-290 nm

decreased with the decreasing lignin content of the pulps. This was expected, since the band at 280 nm has been assigned to originate from residual lignin in the pulp (Schmidt, Heitner 1999). In addition to the decrease in the band intensity, there was a small shift in the band maximum to lower wavenumbers.

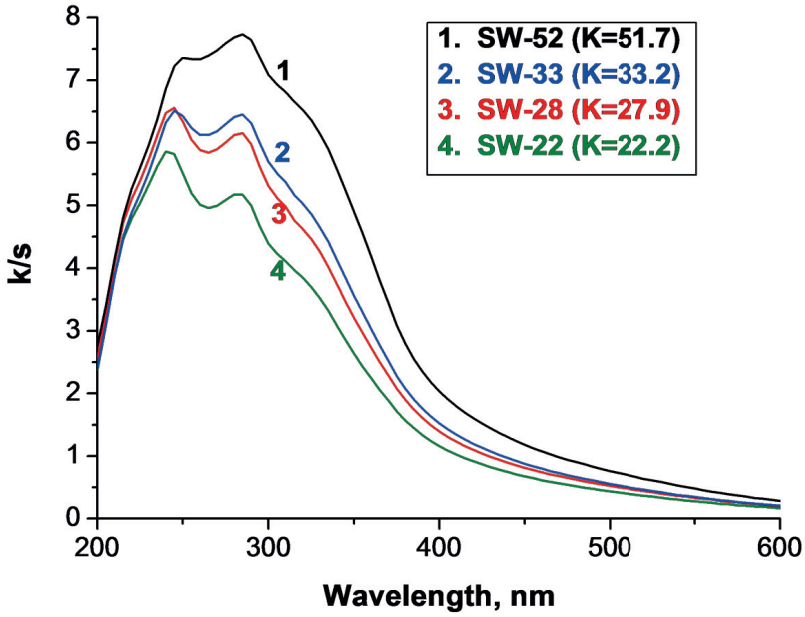

Figure 10. UV-Vis spectra of unbleached softwood (SW) kraft pulps with kappa numbers 22-52. The reflectance spectra were converted into k/s spectra (**Paper I**).

In Figure 10, the height of the band at ca. 240 nm, which has been assigned to hexenuronic acid groups (Ragnar 2001, Liitiä, Tamminen et al. 2004) correlates with the hexenuronic acid group content in the samples (Table 1). However, the overlapping lignin signals influence also the intensity of the signal assigned to HexA. Therefore, various methods to exclude the effects of delignification on HexA removal in UV-Vis were suggested (Ragnar 2001, Liitiä, Tamminen et al. 2004).

The effect of delignification conditions were further studied with UVRR and UV-Vis spectroscopies. For this purpose, two pulps with kappa level 30 were produced either by pulping with low sulphidity (LS) or by using profiled alkali (PA) cooking. In addition, the extended delignification was studied by continuing the profiled alkali cooking to kappa

level 18, or by finishing pulping at kappa level 30, and then continuing the delignification with oxygen to kappa level 18. Differences in the UVRR and UV-Vis spectra of these pulps are shown in Figures 11 and 12.

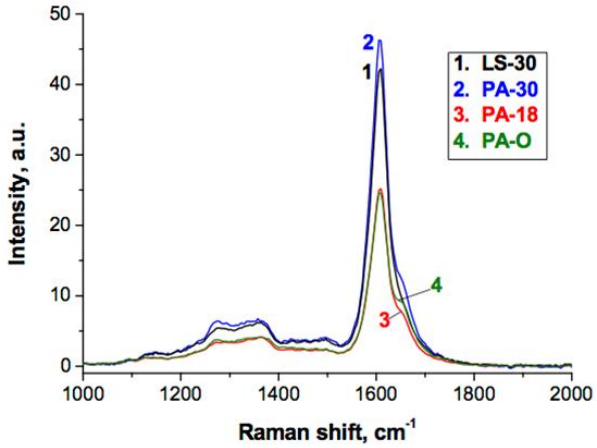

Figure 11. UVRR spectra of low sulphidity pulp at kappa level 30 (LS-30), profiled alkali-cooked pulps at kappa levels 30 and 18 (PA-30 and PA-18, respectively), and profiled alkali-cooked pulp after oxygen delignification at kappa level 18 (PA-O) (**Paper I**).

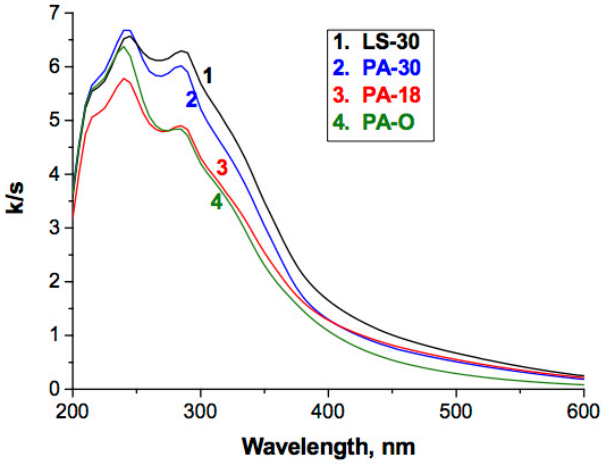

Figure 12. UV-Vis (k/s) spectra of low sulphidity pulp at kappa level 30 (LS-30), profiled alkali-cooked pulps at kappa levels 30 and 18 (PA-30 and PA-18, respectively), and profiled alkali-cooked pulp after oxygen delignification at kappa level 18 (PA-O) (**Paper I**).

Figure 11 depicts how the UVRR spectra the aromatic stretching band at 1605 cm^{-1} was higher for the PA pulp than for the LS pulp, which agrees with the results from the wet chemical analyses (Table 1). Furthermore, the unsaturated band at ca. 1658 cm^{-1} was higher for the PA pulp, which also correlates with the hexenuronic acid content of the pulp (Table 1).

The results from the UV-Vis spectroscopy (Figure 12) were not as straightforward. The band intensity at 280 nm in UV-Vis spectra was higher for LS, with a lower lignin content as measured by kappa number (Table 1). The higher intensity at 280 nm despite the lower lignin content of the LS pulp was probably affected by the different structure and higher absorptivity of LS lignin, which could be seen also as a darker color of LS residual lignin, as reported previously (Liitiä, Ranua et al. 2005). The difference between the LS and PA pulps at wavelength of 240 nm at kappa level 30 was minor, although the HexA content of LS pulp was significantly lower (Table 1). The higher absorptivity of LS lignin probably also reduced the differences observed at 240 nm.

The oxygen delignification did not remove hexenuronic acid groups, which can be seen as a higher band intensity at 1658 cm^{-1} in the UVRR spectra and at 240 nm in the UV-Vis spectra when compared to PA-18 cooked to the same kappa level (Table 1 and Figures 11 and 12). Nevertheless, when the same kappa level was reached by extending the cook to kappa level 18, remarkable degradation of hexenuronic acid groups occurred.

Both UVRR and UV-Vis spectra suggested changes in the residual lignin structure during kraft pulping. Based on the UVRR spectra, accumulation or formation of some structures containing C=C aromatics existed, while UV-Vis revealed reduction in C=O structures. Based on literature (Froass, Ragauskas et al. 1996, Gellerstedt, Lindfors 1984) the residual lignin after a prolonged cooking contains more carboxylic acid groups, more phenolic hydroxyl groups, and more condensed structures than after a short cooking. However, aliphatic hydroxyl (OH) and β-O-4 structures are lower in concentration. The increase in the phenolic hydroxyl group (OH_{phen}) content of residual lignin in the unbleached kraft pulps with decreasing kappa number was indeed observed earlier (Lähdetie, Liitiä et al. 2007).

5.1.2 Semi-bleached pulps

Both UVRR and UV-Vis spectroscopy were utilized to characterize semi-bleached softwood kraft pulps. For the semi-bleached PA pulps, the UV resonance Raman and UV-Vis

spectroscopic results correlated very well when the lignin and hexenuronic acid contents were observed. In all cases (bleaching sequences PA-DE, PA-ODE, PA-OZE and PA-OQP) the lignin content decreased as the chemical dosage increased, as shown by UV-Vis and UVRR spectra and the wet chemical methods in **Paper I**. However, PA-OQP pulps differed from the others, as the hexenuronic acid content was not decreasing when the hydrogen peroxide charge was increased. This is in accordance with the known stability of hexenuronic acid with alkaline hydrogen peroxide.

5.1.3 Fully-bleached pulps

The spectra of fully-bleached PA-OQPPaaP and PA-OQPZP pulps are shown in Figures 13 and 14. Table 2 provides the lignin, hexenuronic acid, and carbonyl group contents determined by the traditional methods.

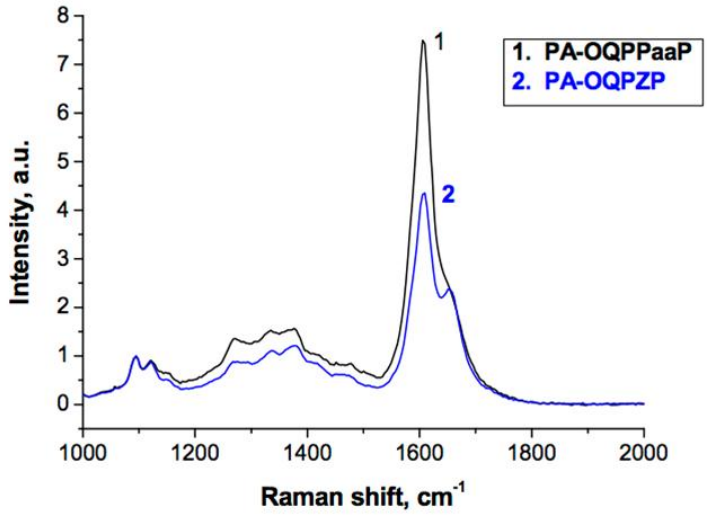

Figure 13. UVRR spectra of PA-OQPPaaP and PA-OQPZP pulps (**Paper I**).

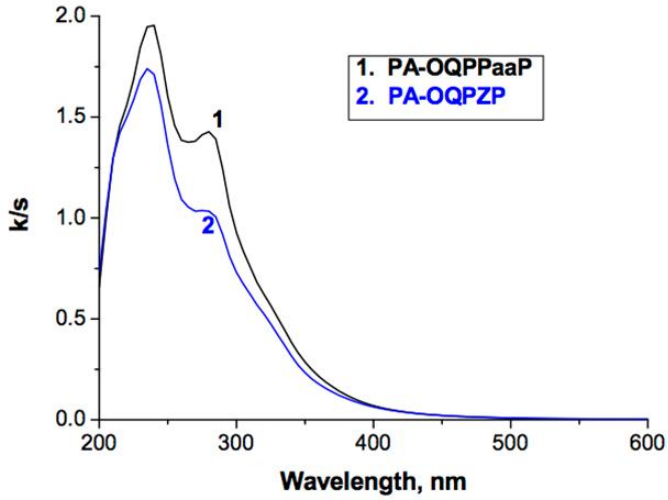

Figure 14. UV-Vis spectra of PA-OQPPaaP and PA-OQPZP pulps, converted into k/s curves (**Paper I**).

Table 2. Kappa number, hexenuronic acid group, lignin and carbonyl group (C=O) content of fully-bleached pulps (**Paper I**).

Sample code	Kappa number	HexA (mmol/kg)	Lignin kappa*)	C=O (mmol/kg)
PA-OQPPaaP	3.7	4.1	3.3	6
PA-OQPZP	3.3	11	2.3	7

*) The lignin kappa number was calculated as the difference between the standard kappa number and the kappa number from HexA.

In the UVRR spectra (Figure 13), the band at 1658 cm^{-1} from hexenuronic acid groups was equally high in both samples, while peracetic acid (Paa) bleached pulp contained notably more lignin than the ozone-treated (Z) pulp. However, the hexenuronic acid content of peracetic acid bleached pulp was much lower than that of ozone-bleached pulp (Table 2). This contradictory result could be due to seriously overlapping bands and, hence, a high lignin content increased also the intensity at 1658 cm^{-1}. The UV-Vis spectra (Figure 14) further revealed the higher lignin content for peracetic acid bleached pulp, but it, moreover, seemed to contain slightly more hexenuronic acid groups than the ozone-bleached pulp. This is, again, due to the effect of higher lignin content and overlapping lignin signals at 240 nm.

The UVRR and UV-Vis spectra of PA-OQPPaaP and PA-OQPZP pulps show that peracetic acid removed hexenuronic acid (relative to lignin) markedly more efficiently than ozone. Nevertheless, ozone removed more lignin structures than hexenuronic acid from the pulp, as shown also by the chemical analyses presented in Table 2 and as stated in the literature (Vuorinen, Adorjan et al. 2007).

5.1.4 Comparison of UVRR and UV-Vis spectroscopy

As was illustrated above, both UVRR and UV-Vis spectroscopy revealed changes both in residual lignin and hexenuronic acid content in pulps. It has been well documented that the lignin content of a sample is directly proportional to the intensity of the aromatic stretching band of the UVRR spectrum (Jääskeläinen, Saariaho et al. 2005) and the absorbance of the UV-Vis spectrum (Schmidt, Heitner 1999). Hence, the results obtained by these two methods were compared.

In order to determine the height of the Raman bands, the spectra were deconvoluted to minimize the influence of partly overlapping bands. An example of the deconvolution is shown in Figure 15. This way the heights of the bands at 1605 cm^{-1} and 1658 cm^{-1} could be defined without a remarkable interference from the neighboring bands.

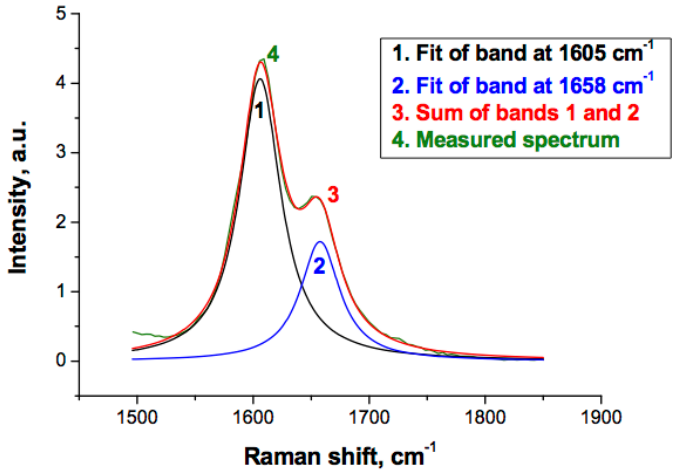

Figure 15. Least-square fit of Lorentzian curves in the spectral range of 1500-1700 cm^{-1} for a PA-ODEDP sample (**Paper I**).

However, the UV-Vis spectra were not deconvoluted, because the number of components in the spectra and their band height maxima could not be defined with good repeatability. Hence, the absorbances at the band maxima of the UV-Vis spectra were defined directly from the spectra.

The comparison of the absorbance of the UV-Vis band at 280 nm and intensity of the UVRR band at 1605 cm^{-1} showed an adequate correlation, as illustrated in Figure 14. Only at a high lignin content, the deviation between Raman and UV-Vis spectroscopy increased remarkably.

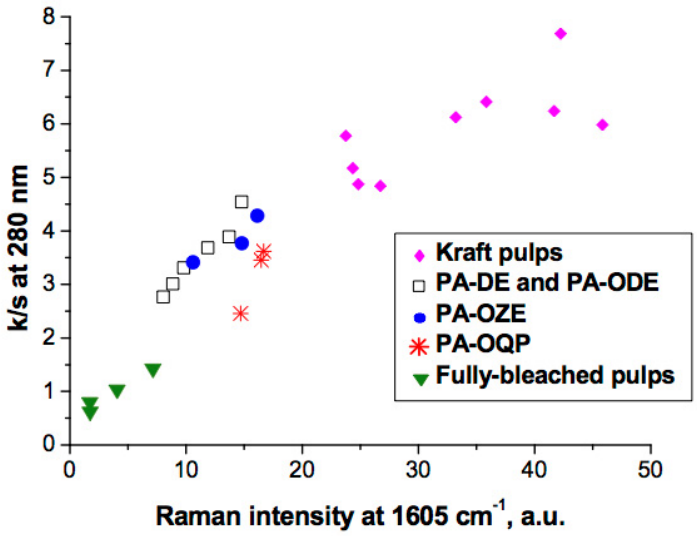

Figure 16. Correlation of UV-Vis absorption band at 280 nm to Raman band at 1605 cm^{-1} (**Paper I**).

The increased deviation at high lignin content may be partly due to the saturation of UV-Vis spectra of the unbleached pulps and, hence, a linear correlation of the absorbance with the lignin content no longer exists (Liitiä, Tamminen et al. 2004). Some deviation in the UVRR band height determination could also be expected, because the cellulose band in the UVRR spectra of unbleached kraft pulps was only a few times as high as the spectral noise. Therefore, the spectral normalization to this band may induce a large deviation in the band height at 1605 cm^{-1}. Despite of these limitations, both of these techniques produced similar results and, thus, are well applicable for samples with low lignin content.

The correlation of the unsaturated stretching band for hexenuronic acids at 1658 cm^{-1} in the UVRR and the absorbance at 240 nm in the UV-Vis spectra was found to be only indicative (Figure 17). The correlation was moderate for the fully- and semi-bleached pulps, excluding the peroxide-bleached (PA-OQP) pulps, whereas the unbleached pulps showed practically no correlation.

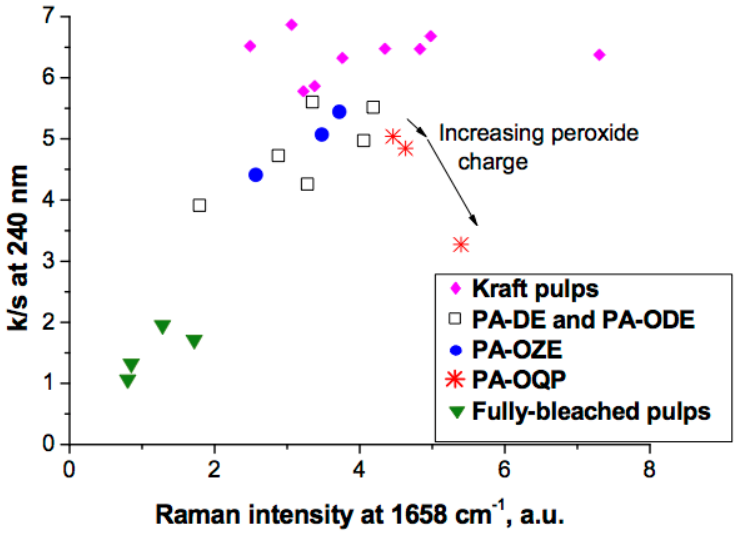

Figure 17. Correlation of UV-Vis absorption band at 240 nm to Raman band at 1605 cm^{-1} (**Paper I**).

The poor correlation between these bands can be explained by the contribution of other pulp structures at these spectral regions. In the UV-Vis spectra, the signal intensity at 240 nm is influenced by the pulp lignin content, because lignin has absorbance also in this range (Ragnar 2001, Liitiä, Tamminen et al. 2004).

The UVRR band at 1658 cm^{-1} was also influenced by other structures in addition to hexenuronic acid. It has been observed that hexenuronic acid groups give rise to a band at 1655 cm^{-1}, as it has been defined with hexenuronic acid model (Adorjan, Jääskeläinen et al. 2006) and pulps with a high amount of hexenuronic acid groups (Jääskeläinen, Saariaho et al. 2005). However, in this study the deconvoluted UVRR spectra revealed the band maximum at 1658 cm^{-1}, which is at higher wavenumbers than that of hexenuronic acid. In addition, a notable band was present also in pulps with practically no hexenuronic acid

groups (Figure 15). The presence of other structures affecting this band is also shown in Figure 18, where the deconvoluted Raman band intensity at 1658 cm^{-1} was plotted against the hexenuronic acid content of the pulps as measured by wet chemical methods. Since the 1658 cm^{-1} band intensity was ca. 0.8 a.u. for the pulps with no detectable amount of hexenuronic acid groups, it is obvious that also other substances contribute to this band.

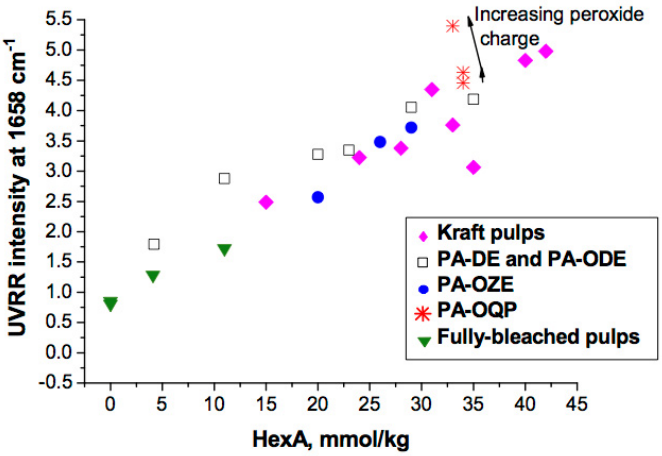

Figure 18. Correlation of the intensity of the deconvoluted UVRR band at 1658 cm^{-1} nm with hexenuronic acid group content of the pulps (**Paper I**).

UV resonance Raman spectroscopy is a valuable technique in lignin analysis *in situ* for samples with a low lignin content. The lignin content determination was fast also with UV-Vis spectroscopy, and only small amounts of sample and little sample preparation were required. In addition, these two spectroscopic techniques correlated well for semi- or fully-bleached pulps. However, samples with higher lignin content (unbleached pulps) showed much more variance. This was possibly due to saturation of UV-Vis spectra and low intensity of the internal standard band (at ca. 1098 cm^{-1}) in the UVRR spectra.

Hexenuronic acid group determination by these techniques showed much more variance. For certain semi- and fully-bleached pulps a relatively good correlation was observed, while unbleached and peroxide-bleached pulps showed clearly scattered data. The height of the deconvoluted UVRR band at 1658 cm^{-1} correlated well with the measured hexenuronic acid group content of the samples, even if it is probable that also other structures in pulps affected this band.

5.2 Activation of thermomechanical pulp lignin by laccases

Fiber functionalization is a method used to produce fibers with significantly altered properties. In such a process, the fiber surfaces are first activated and then the reaction with other compounds follows (functionalization). The activation can be carried out by radicalization, i.e., forming radicals on the surface, followed by radical coupling of the other compound (Felby, Pedersen et al. 1997, Grönqvist, Buchert et al. 2003). Laccases are oxidative enzymes suited for the activation of lignin-containing fibers before functionalization. Laccases need molecular oxygen for oxidizing various aromatic and non-aromatic compounds by a radical reaction mechanism (Claus 2003, Claus 2004). Phenolic hydroxyl groups (OH_{phen}) in lignins – as an essential part of fibers – are oxidized to phenoxy radicals that are ready for functionalization. This is one of the strategies to modify the properties of thermomechanical pulp (TMP) (Grönqvist, Rantanen et al. 2006).

The laccase treatment polymerizes and degrades phenolic lignin structures via radical mechanism (Niku-Paavola, Karhunen et al. 1988, Grönqvist, Viikari et al. 2005): lignins with small molecular weight are mainly polymerized, whereas lignins with large molecular weight are mainly degraded (Niku-Paavola, Tamminen et al. 2002, Rittstieg, Suurnakki et al. 2002). Laccases also lead to the polymerization of lignans (Buchert, Mustranta et al. 2002). Hence, laccases can be considered as activation agents in fiber functionalization (Grönqvist, Rantanen et al. 2006).

The chemical changes induced by laccases of *Trametes hirsuta* (ThL) and *Melanocarpus albomyces* (MaL) in TMP lignin were observed using spectroscopic methods. The basic difference between these laccases is in their redox potential (Kiiskinen, Viikari et al. 2002). In addition, it has been observed that the lignin surfaces activated by ThL followed by the attachment of polymerized ferulic acid were more stable than the corresponding surfaces activated by MaL (Saarinen, Suurnäkki et al. 2009). Hence, to gain information on the chemical changes during the laccase treatment and to clarify the difference between ThL and MaL, TMP was activated with these laccases and followed by UV resonance Raman (UVRR) spectroscopy. Additionally, reflectance UV-Vis and FTIR spectroscopic techniques were used to monitor the activation and to compare the results to Raman spectroscopy.

The laccase treatment decreased the brightness (measured as reflectance values with UV-Vis spectroscopy) of the TMP samples. A long laccase treatment resulted in a lower brightness than a short laccase treatment. The brightness decreased with both MaL and

ThL laccases, but it remained slightly higher with MaL than with ThL. The decreased brightness of laccase-treated pulps is in agreement with findings by other researchers (Chandra, Beatson et al. 1999, Petit-Conil, Semar et al. 2002).

The brightness was remarkably lower at the wire side than at the upper side of the handmade pulp sheet. This can be explained by the uneven distribution of fines in the pulp sheet. It is obvious that the upper side contains fewer fines than the wire side, and hence the light scattering properties of the sides are different. Fines have different scattering properties than fibers, and are known to be enriched by lignin and extractives (Luukko 1998, Kleen, Kangas et al. 2003); accordingly, fines have a lower brightness than fibers.

The greatest effect of the activation was observed with the longest treatment time (100 min) for both ThL and MaL. The UV-Vis reflectance and k/s absorbance spectra of TMP pulps with this treatment time are presented in Figure 19. Only a minor effect was observed after 1 and 10 min.

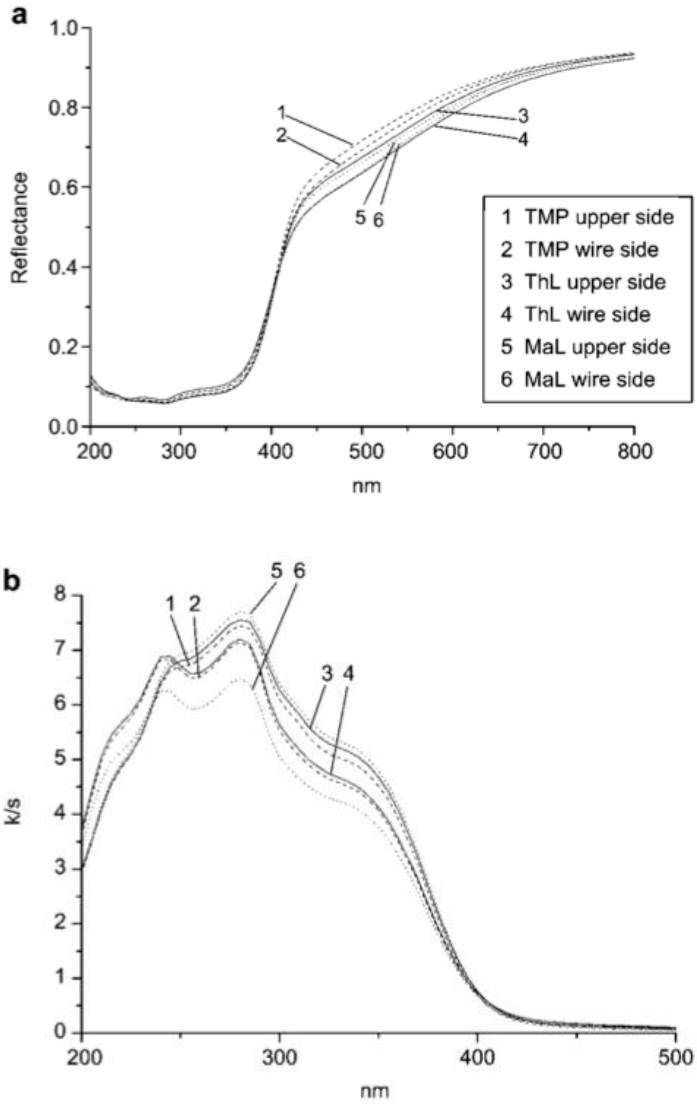

Figure 19. (a) UV-Vis reflectance spectra and (b) k/s absorbance spectra of the reference (TMP) and laccase treated (ThL and MaL) pulps as measured from the upper and the wire side of the pulp sheets. Reference and laccase treatment time was 100 min (**Paper II**).

The spectra in Figure 19a reveal that the laccase treatment darkened the sample in the entire visible spectral range. The reflectance spectra were also less intense on the wire side of the sample than on its upper side. To gain more structural information, the UV-Vis

spectra were converted to absorbance (k/s) spectra (Figure 19b). The spectra from the wire side were clearly different from that of the upper side. The effects of the laccase treatment were less significant than those caused by the two sides of the sheet.

All Raman spectra were baseline-corrected, and the band heights were normalized to the highest band at approximately 1605 cm^{-1} (= a.u.). In the UVRR spectra collected at 244 nm excitation wavelength, the differences between the laccase treated pulps were very small and below the level of significance (Figure 20). The influence of the sides was not significant, either. Accordingly, the fines structure or the fines content have no remarkable impact on the UVRR spectral analyses.

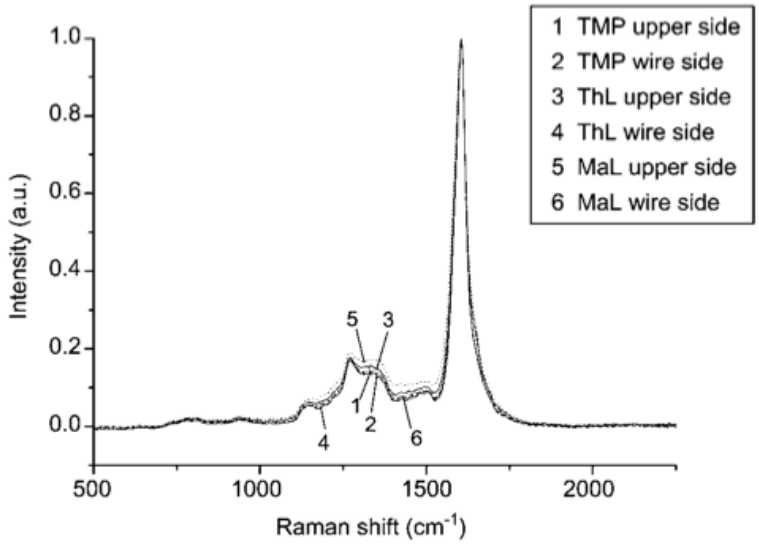

Figure 20. UVRR spectra collected at 244 nm of the pulps treated for 100 min from different sides of the pulp sheets. TMP, reference pulp; MaL and ThL, laccase-treated pulps (**Paper II**).

In order to minimize the impact of the uneven distribution of the fines in the z-direction of the samples, the fines were separated from the TMP samples treated for 100 min. After the separation, the upper side and the wire side of the pulp sheets were almost identical, deviating only less than 1% unit in brightness, and showing only minor deviation between the upper and the wire side of the fractionated fibers by UV-Vis spectroscopy.

The UV-Vis k/s absorbance spectra of the fiber fractions of the reference and the laccase-treated pulps are presented in Figure 21a, and the UVRR spectra of the pulps collected at 257 nm excitation wavelength are presented in Figure 21b.

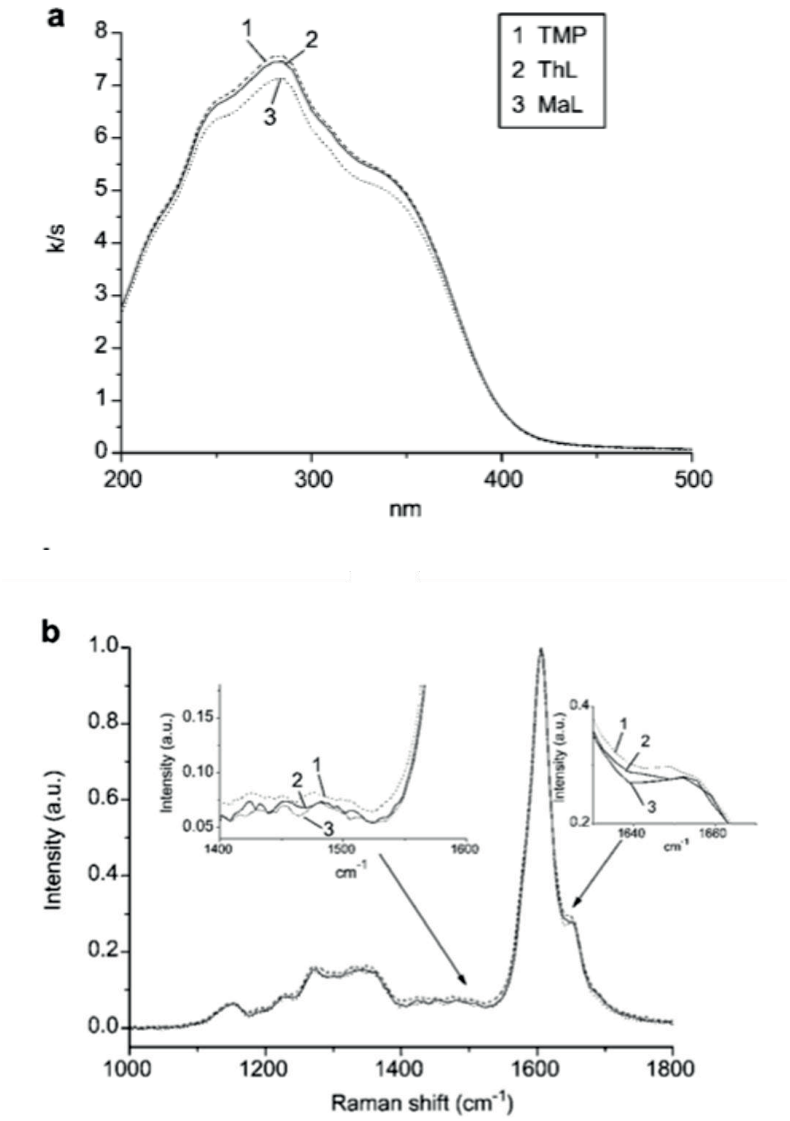

Figure 21. (a) UV-Vis spectra and (b) UVRR spectra collected at 257 nm of fiber fractions of 100 min treated pulps (**Paper II**).

When the fines were removed, the UV-Vis absorption bands at ca. 265, 280 and 350 nm originating from fiber fraction are resolved (Figure 17a). For comparison, the wire side of the samples emphasized the bands at approximately 210 and 240 nm (Figure 19), indicating the presence of a higher number of carbonyl groups and unsaturated structures in fines than in the fiber fraction (Liitiä, Tamminen et al. 2004).

The UV-Vis spectra show that only minor structural differences between the two laccase treated TMP fibers were present. The subtraction spectra illustrated that MaL removed more structures that absorb at approximately 300–330 nm. However, these detected changes were only minor, and the results can be affected by the saturation of UV region due to the very high lignin content of mechanical pulps, as well as by possible changes in scattering.

In the UVRR spectra measured at 257 nm excitation wavelength (Figure 21b), the aromatic band at approximately 1605 cm^{-1} was very high due to the high lignin content in TMP. When the pulp was treated with laccase, the relative intensity of the band arising from unsaturated structures at approximately 1650 cm^{-1} decreased more notably with MaL. This Raman spectral range originates mainly from the unsaturated stretching mode of coniferyl alcohol, while carbonyl stretching mode of coniferyl aldehyde may also have an influence in this spectral range (Agarwal, Ralph 2008). However, unsaturated extractives may have bands in this range as well (Nuopponen, Willför et al. 2004). The UVRR results support those from the UV-Vis spectral data, and demonstrate that the amount of conjugated structures decreased in the fiber fraction during the MaL treatment.

The FTIR spectra of the laccase-treated samples and the TMP reference sample were almost identical. The lignin contents of the laccase-treated samples were slightly lower than those of the reference sample, which correlates with the results of the UV-Vis spectroscopy.

Although pulp brightness was reduced by the laccase treatment of spruce TMP, the spectroscopic methods showed only small structural differences in laccase treated TMP. UVRR and UV-Vis spectroscopies revealed that MaL had a more significant effect on the lignin structure and/or content than ThL, though its redox potential is lower (ThL 750 mV > MaL 470 mV). MaL is known to have a stronger tendency to adsorb on the fiber surface, while ThL is capable of forming a more stable aggregation of substances on lignin surfaces (Saarinen, Suurnäkki et al. 2009). The pulp brightness remained higher after the MaL treatment than after the ThL treatment. MaL seems to be a promising enzyme for fiber functionalization. The lower brightness reduction may be partly due to the lesser

tendency of MaL to recondense dissolved lignan/lignin material onto the fibers. This effect was confirmed by UV-Vis spectroscopic measurements of the reaction filtrates.

The variations between the differently activated TMP samples were relatively small in UV resonance Raman spectroscopy. Due to the high lignin content of TMP, the resonance enhanced aromatic band at ca. 1605 cm^{-1} was very high, and it was more challenging to observe differences in other, less intense, Raman bands between different samples.

5.3 Effect of pH on lignin analysis by Raman spectroscopy

The analysis of the lignin structure is challenging because of the complexity of the macromolecule itself, its limited solubility, and covalent bonding to carbohydrates inside the plant cell wall. The isolation of lignin from the biomass introduces changes, regardless of the isolation method applied; it alters the amount of functional groups, which may be crucial for lignin reactivity. Therefore, an *in situ* analysis is preferable, and more likely to reveal the true features of lignin.

A quantitative analysis with Raman spectroscopy is most commonly based on the proportional relationship between Raman scattering intensity and the analyte concentration (Pelletier 2003). This way it is possible to determine, for example, lignin or hexenuronic acid content in pulps (Halttunen, Vyörykkä et al. 2001, Saariaho, Hortling et al. 2003, Jääskeläinen, Saariaho et al. 2005). However, the changes in Raman shifts and band shape are also suitable for qualitative and quantitative analysis (Chi, Chen et al. 1998, Wu, Nelson et al. 2000).

Knowledge of the functional groups of lignin is of great importance as they contribute largely to various properties of ligneous materials. Phenolic hydroxyl groups (OH_{phen}) are the most essential functional groups and responsible for the reactivity of lignin and its solubilization in pulping and bleaching (Adler, Hernestam 1955, Zakis 1994, Lapierre, Pollet et al. 1999, Sjöström, Alen 1999). However, hydroxyl and carboxylic acid groups are easily functionalized and this affects the compatibility of lignin with different polymers (Doherty, Mousavioun et al. 2011). Moreover, the potential of lignin to be engaged in free radical co-polymerization with unsaturated polymers depends on the ability of OH_{phen} groups to act as radical scavengers (Barclay, Xi et al. 1997). Additionally, radical-scavenging action of phenolic structures generates antioxidant properties of the lignin polymer itself (Dizhbite, Telysheva et al. 2004).

Recently, new methods to quantify phenolic hydroxyl groups in pulps without isolating lignin were developed (Warsta, Jääskeläinen et al. 2006, Eshkiki, Mortha et al. 2007, Liitiä, Tamminen 2007, Delmas, Lachenal et al. 2009). An application of UV resonance Raman (UVRR) and UV-Vis spectroscopic methods for this purpose is based on ionization of OH_{phen} in alkaline media, which introduces recordable shifts in spectral bands. These methods produced similar results (Lähdetie, Liitiä et al. 2007).

The effect of pH on UVRR spectra of lignin model compounds and wood pulps was observed, in order to confirm that the detected shift in aromatic Raman bands is derived from the ionization of the OH_{phen} groups. The study was completed with a series of monomeric lignin model compounds in aqueous solutions as a function of pH and concentration. In this approach, the most considerable advantages of Raman spectroscopy were utilized: its insensitivity towards water and the variability of the sample forms that are suitable for measurements (Sjöström, Alen 1999, Pelletier 2003).

A variety of model compound concentrations were tested, and it was observed that approximately 1 mM concentration was the lower quantification limit in the UVRR setup with the sodium sulfate standard. Below this concentration the low signal to noise (S/N) ratio impeded the recording of high-quality spectra.

All spectra indicated the same trend: a clear shift of the aromatic band towards lower wave numbers was detected when the pH was changed from neutral to alkaline. The UVRR spectra of phenol and p-cresol are shown in Figure 22.

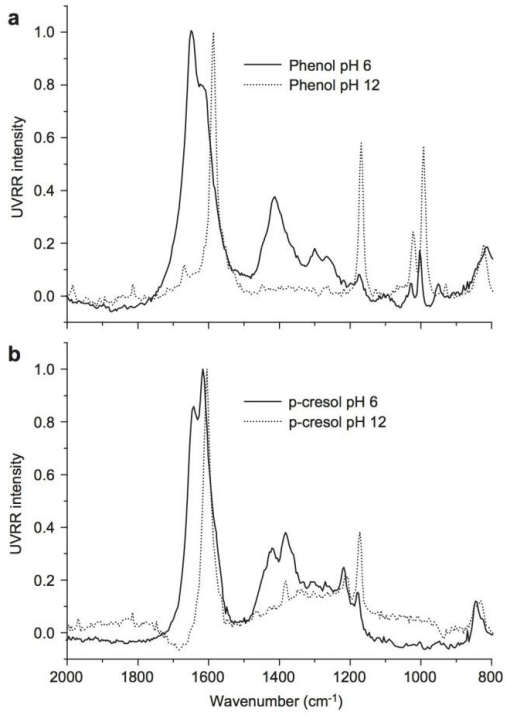

Figure 22. Ultraviolet resonance Raman (UVRR) spectra of (a) phenol and (b) p-cresol in solution. The spectra are baseline corrected to zero at 800 and 2000 cm^{-1}, and the buffers are subtracted from the spectra. The spectra are normalized to highest intensity, but these samples did not include an internal standard, i.e., the intensity values are random (**Paper III**).

The shifts in the spectra of model compounds were much larger (8-35 cm^{-1}) than the ones collected from pulp samples (approx. 2-7 cm^{-1}) (Warsta, Jääskeläinen et al. 2006, Lähdetie, Liitiä et al. 2007). The greater shift can be explained by the fact that each model compound has an OH_{phen}, while in pulp only some of the aromatic rings contain these phenolic hydroxyl groups. The model compounds with methyl or propenyl group in the *para* position induced substantially smaller shifts (8-12 cm^{-1}) compared to the model compounds without the *para* substituent (25-35 cm^{-1}).

The UVRR spectra of the model compound solutions with an internal standard or ethanol revealed that the pH has a substantial effect on the intensity of the Raman band. Increasing the pH increased the intensity of the aromatic bands. The pH-induced shift in

the spectra was not dependent on the model compound concentration, as discovered from the measurements of the concentration series of guaiacol. However, the intensity of the aromatic band was proportional to the concentration of guaiacol: the intensity of the band increased when the concentration increased.

As the model compounds without the *para* substituent had markedly greater shift in the aromatic band position (>25 cm^{-1}), and the model compounds with the *para* substituent resulted a shift close to the ones obtained from pulp samples, it is suggested that the spectra of the latter compounds are more relevant in pulp lignin structure studies. On the basis of these results, the shift of the aromatic band from neutral to alkaline in a UVRR spectrum indicates the amount of phenolic hydroxyl groups. Thus, if all lignin phenylpropane units have a free OH_{phen}, the shift in the spectrum is ca. 11 cm^{-1}. The aromatic band position at pH 6 may give a hint of the structural differences in lignin samples, as the position is shifted towards lower wave numbers (1617-1606 cm^{-1}), when the degree of substitution and the number of conjugated double bonds is increased. Additionally, *p*-substituted structures induced a band at around 1550-1560 cm^{-1}.

The model compound measurements confirmed that liquid lignin samples can be quantitatively evaluated by the use of UVRR spectroscopy combined with an internal standard. Nevertheless, the pH of all samples should be set prior to measurements, because it influences the intensity and the position of the Raman bands. More structural information is obtained at an alkaline pH.

5.4 Laser-induced fluorescence of lignin in Raman spectroscopy

The major drawback in using Raman spectroscopy is the simultaneously emitted laser induced fluorescence (LIF) (Conners 1995, Agarwal 1999). LIF overlaps with Raman bands, and this background signal can in the worst case overwhelm the weaker Raman signal completely. Hence LIF obstructs the sample characterization, and restricts the use of Raman spectroscopy when the excitation energy falls in the UV-Vis range.

The laser induced fluorescence of lignin in Raman spectroscopy was investigated using visible laser excitation (532 nm, green laser). Fluorescence and UV-Vis absorbance spectroscopic techniques were also used to further investigate the fluorescence properties of lignin model compounds.

Several different lignin model compounds were studied using Raman spectroscopy with the excitation wavelength of 532 nm. The spectra were neither normalized nor baseline-

corrected in order to study and compare the backgrounds and signal intensities of the spectra.

The model compounds in Figure 1 represent the most typical lignin structures. Erol [**1**] is a dimer only with a β-O-4 linkage and bierol [**2**] is its tetramer, in which two erols are linked via 5-5′ linkage. Dibenzodioxocin [**3**] is an etherified biphenyl unit with a guaiacylpropan; it contains the 5-5′ linkage as well as an eight-membered ring structure. 4-O-methylated bierol [**4**] is derived from compound [**2**] by methylation of the phenolic hydroxyl groups. (Figure 23).

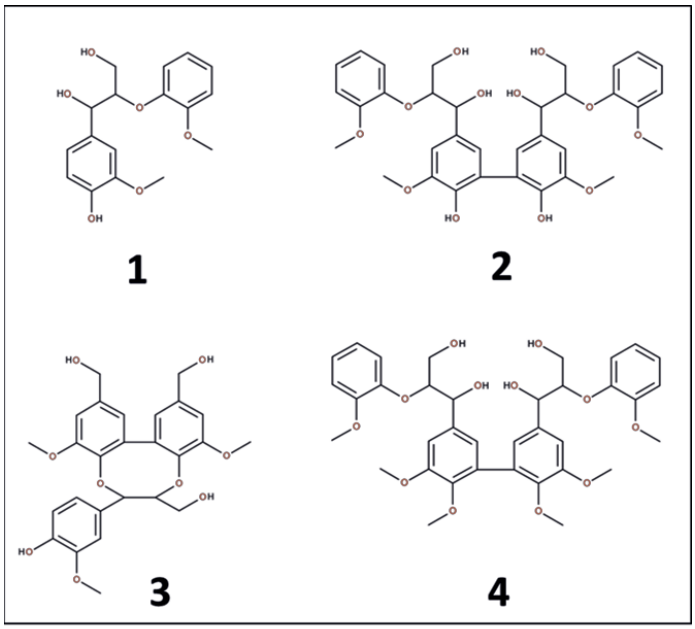

Figure 23. Structural formulas of erol [**1**], bierol [**2**], dibenzodioxocin [**3**], 4-O-methylated bierol [**4**].

Figure 24 shows the Raman spectra of the model compounds.

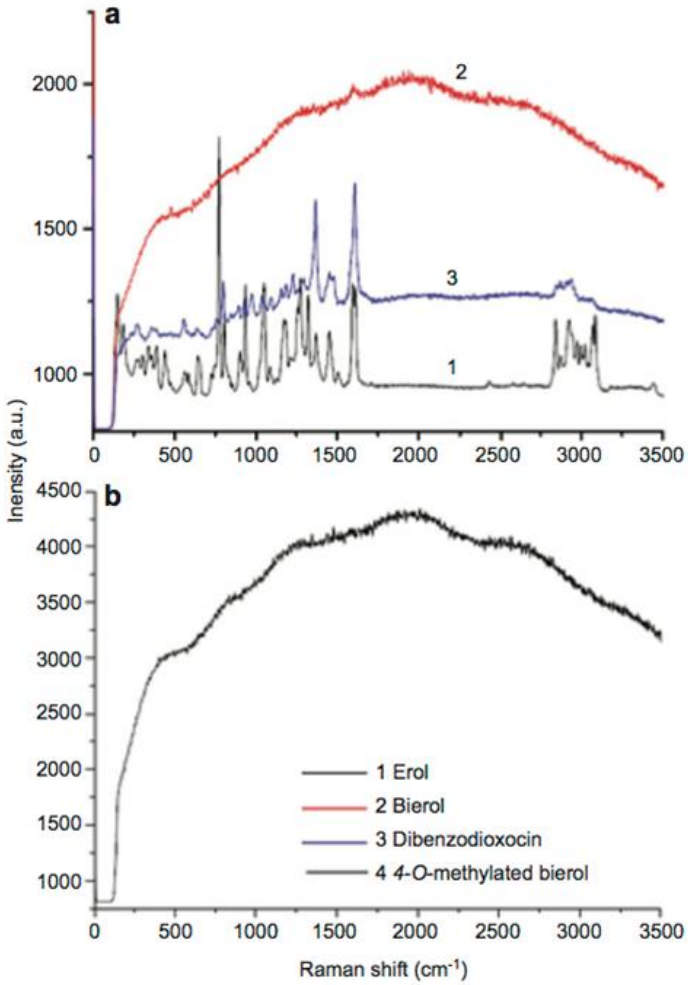

Figure 24. Raman spectra of a) erol [**1**], bierol [**2**] and dibenzodioxocin [**3**], and b) 4-O-methylated bierol collected at 532 nm excitation (**Paper IV**).

Figure 24a indicates that erol produced a very clear Raman signal when excited with 532 nm excitation wavelength. The peaks of the spectrum were narrow and the baseline was flat. However, the spectrum of bierol had a strong fluorescing background which swamped the Raman bands almost completely. Only a weak and broad band at ca. 1600 cm^{-1} arising from the aromatic stretching mode could be identified in the spectrum. The only structural difference between erol and bierol lies in the size of the molecules and in the 5-5' linkage. Thus it can be concluded that the fluorescence in the Raman spectrum of bierol arises from the 5-5' linkages via the conjugation system over the two aromatic rings.

Figure 24a further shows the Raman spectrum of dibenzodioxocin [**3**], which is a condensed lignin substructure. This signal was clear, and it did not have notable fluorescence disturbing the Raman analysis. Although dibenzodioxocin contains the same 5-5' linkage as bierol, the rigid conformation with the octagonal ring of the molecule seems to decrease the contribution of LIF to the Raman spectrum.

The situation is very different in the Raman spectrum of bierol [**2**] and 4-O-methylated bierol [**4**] in Figure 24: the very intense fluorescence emission masks the Raman components of the spectrum. This observation is interpreted that the presence of the substantially freely rotating 5-5′-type aromatic structure is the prerequisite for LIF.

In order to obtain more detailed information on fluorescence properties of the model compounds, fluorescence spectra were collected from erol [**1**], bierol [**2**] and dibenzodioxocin [**3**]. The spectra of the model compounds with excitation wavelength of 532 nm are depicted in Figure 25.

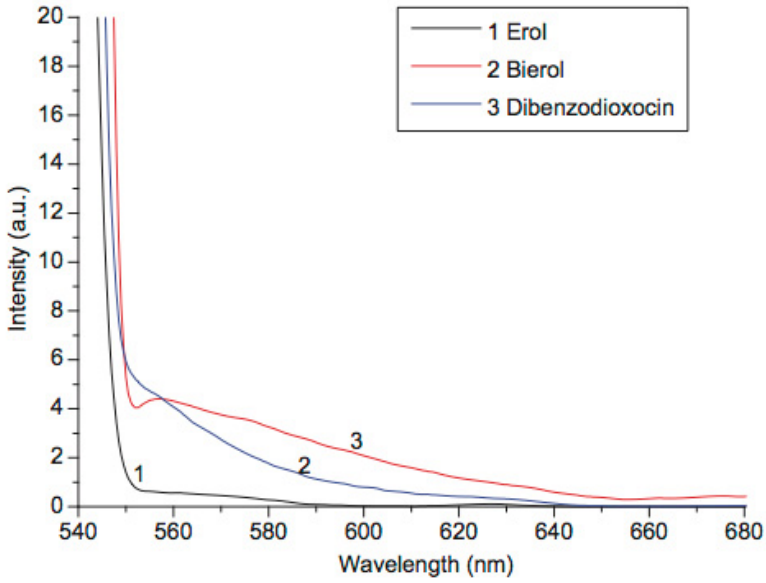

Figure 25. Fluorescence spectra of bierol, erol and dibenzodioxocin collected at 532 nm excitation (**Paper IV**).

Figure 25 shows that all model compounds emitted some fluorescence when excited with 532 nm excitation wavelength. Nevertheless, the level of fluorescence of erol was very small, and it could be detected only within the range from ca. 550 to 590 nm (Figure 25).

This wavelength area corresponds to the wavenumber range from ca. 615 cm^{-1} to 1850 cm^{-1} in the Raman spectrum. However, in the Raman spectrum of erol no fluorescence was present to disturb the analysis within this range (Figure 24a). Only a small fluctuation of baseline could be seen, and otherwise the distinctive Raman bands were clearly visible.

The fluorescence spectrum of dibenzodioxocin showed that it emitted considerably more fluorescence than erol within the range from ca. 550 to 645 nm (Figure 25). This corresponds to the wavenumber range from ca. 615 cm^{-1} to 3300 cm^{-1} in the Raman spectrum. Indeed, dibenzodioxocin had a moderate fluorescence background within this range in its Raman spectrum (Figure 24a). Nevertheless, this amount of fluorescence did not disturb the analysis, and the Raman bands were clear and visible also for dibenzodioxocin.

Bierol had again the highest amount of the emitted fluorescence in Figure 25. It had the most intense emission from ca. 560 to 680 nm, corresponding to the wavenumber range from ca. 940 cm^{-1} to over 4500 cm^{-1}. Interestingly, the intensity of fluorescence emission of bierol was smaller than the intensity of dibenzodioxocin between 550 nm and 558 nm (between 615 cm^{-1} and 875 cm^{-1} in Raman spectrum). However, the Raman signal of dibenzodioxocin is still much clearer also within this range (Figure 24a).

The discrepancy between the low contribution of fluorescence in the Raman spectra and a pronounced fluorescence in the fluorescence spectra with 532 nm excitation agrees with the earlier observations of Meyer et al. (2011). The quoted authors reported that lignin can exhibit strong fluorescence background in Raman spectra even when excited with low energy at 785 nm. Although the LIF measurements do not correlate well with the LIF background of the Raman spectra, the trends are the same and support the hypothesis of the crucial role of conformational aspects. The most relevant conclusion is that the planar 5-5′ structures are powerful inducer of fluorescence.

Fluorescence is usually not such a big problem for chemically untreated wood in Raman spectroscopy. Lignin in wood is in its native form, and the substructures in lignin polymer chains remain intact surrounded by the matrix, i.e. other components of wood. The spectra of spruce wood and spruce fiber (TMP) produced by thermomechanical pulping are very similar. The mechanical treatment does not produce fluorescence background in the Raman spectrum. However, the effect of fluorescence is striking when wood is treated chemically under alkaline conditions (Figure 26).

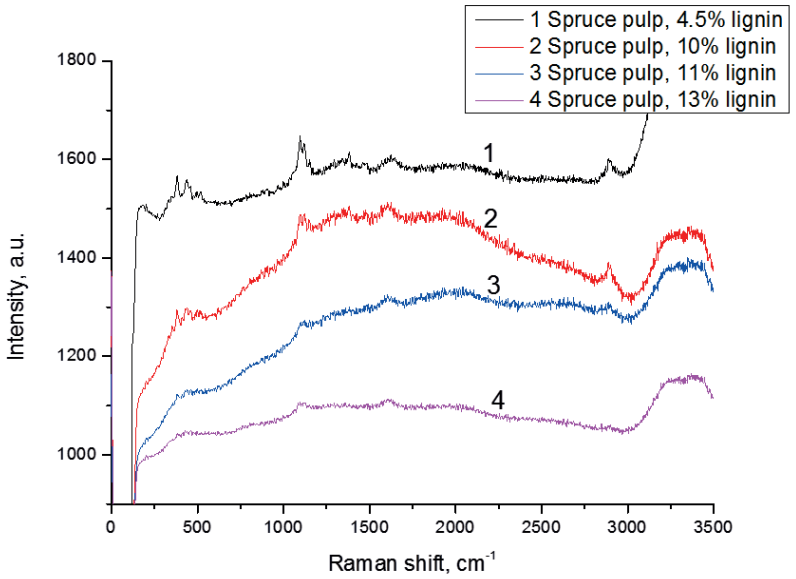

Figure 26. Raman spectra of spruce kraft pulps with lignin content of 4.5%, 10%, 11% and 13% (**Paper IV**).

The Raman bands from cellulose (1098 cm^{-1}) or lignin (1600 cm^{-1}) are very weakly detected in the spectra of the three spruce pulps which have a relatively high lignin content of 10-13%. Obviously LIF diminishes when the lignin concentration in the sample decreased. The Raman signal from a pulp sample is distinctive when the lignin content is only about 4.5%. One reason for the fluorescence emission of the alkaline treated pulp samples could be the cleavage of α- and β-aryl ether bonds in dibenzodioxocin structures in lignin. When the most easily breaking structures are cleaved, more fluorescence seems to be arising from the remaining structures, e.g. the 5-5' biphenyl structures.

Furthermore, different polymeric lignin polymers were studied using Raman spectroscopy in order to determine how well these lignin models represent the structure of native lignin. The Raman spectra of different lignins are shown in Figure 27.

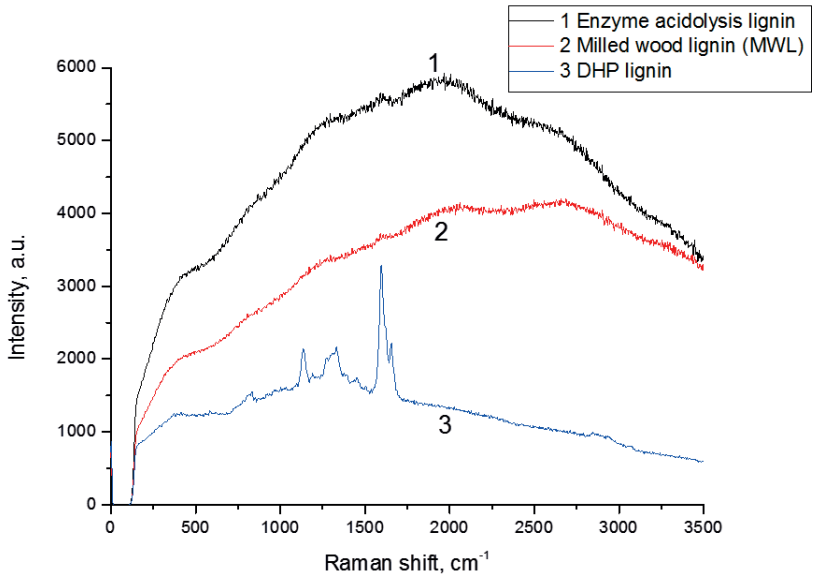

Figure 27. Raman spectra of enzyme acidolysis lignin from kraft pulp, milled wood lignin (MWL) from wood and synthetic DHP lignin (**Paper IV**).

Interestingly the lignin isolated by an enzymatic mild acidolysis (EMAL) procedure produced LIF that swamped all Raman signals completely (Figure 27). The effect of LIF became dominant also when the mechanically isolated milled wood lignin (MWL) was studied. The fluorescence background signal of the MWL in Raman spectrum was overwhelming in Figure 27. MWL and EMAL procedures have been considered methods which alter the lignin structure much less than the other isolation methods, and thus retain the native structure as closely as possible (Fujimoto, Matsumoto et al. 2005). Therefore it is somewhat surprising that these lignins have the fluorescence background in their Raman spectra, as the native lignin in spruce wood sample does not fluoresce greatly. This implies that the native lignin in wood is bound to the matrix in such a way that it prevents fluoresce emission. MWL and EMAL are not bound to carbohydrates, and this, most probably, enables fluorescence emission to occur in those samples.

However, the Raman signal was well visible in the spectrum of a synthetic lignin, dehydrogenation polymer (DHP). The DHP lignin was synthetized from coniferyl alcohol monomeric units. Previously it has been reported that DHP lignins are highly fluorescent (Agarwal, Terashima 2003). However, when compared to enzymatic acidolysis lignin or MWL, the DHP lignin fluoresces the least with the used 532 nm excitation wavelength.

This indicates that the structure of DHP polymer differs profoundly from the native lignin in respect to structures responsible for the LIF.

These results provide significant insight for lignin structural characterization. The role of 5-5' linkages as a source of laser induced fluorescence in Raman spectroscopy has an importance when investigating the structure of lignin.

5.5 Effect of excitation wavelength on the Raman spectra of wood-based samples

The selection of appropriate excitation wavelength is an important factor in Raman spectroscopy. The intensity of Raman scattering is proportional to the incident frequency to the fourth power. Since Raman scattering is a weak effect, a powerful excitation source is needed to provide a high power density at the sample. This can cause a fluorescence emission to occur, especially in the visible region. However, when the frequency of the laser beam is close to the frequency of an electronic transition, Raman scattering enhancements of up to 10^6 can be obtained (Smith, Dent 2005).

In order to see the effect of excitation wavelength on the Raman spectra of different wood-based samples, different lasers at various Raman instruments were used to obtain excitation ranging from ultraviolet (UV) to near infrared (NIR) radiation. This range covers the mostly used excitation wavelengths in Raman spectroscopy, excluding only the longest infrared wavelengths (e.g. 1064 nm). The Raman spectra were measured using nine different excitation wavelengths: 229, 244, 257, 325, 442, 514, 532, 633 and 785 nm. Several wood and pulp samples were used for measuring Raman spectra using all nine different wavelengths.

Figure 28 shows Raman spectra of cellulose, measured with excitation wavelengths from ultraviolet (UV) to near infrared (NIR) range. The spectra were normalized to the cellulose band at ca. 1095 cm^{-1}.

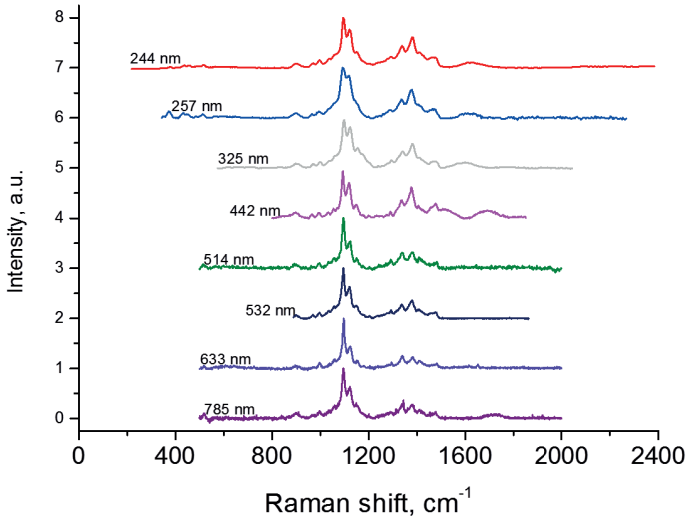

Figure 28. Raman spectra of cellulose. The spectra were offset for the clarity of the figure (**Paper V**).

In general, cellulose is a weak Raman scatterer, hence, there was a small amount of noise in the spectra. All spectra had the same Raman bands in the spectral range of 800-1500 cm^{-1}. However, the relative intensities varied slightly. One reason for the variance can be the changes in the fiber orientation of the samples. In each measurement the samples were placed on the sample table a bit differently, and in measurements with UV excitation (229, 244 and 257 nm) the samples were spun on the sample table to avoid burning. This changed the cellulose orientation and causing small changes in the relative intensities of the bands (Wiley, Atalla 1987). Also the different degrees of polarization of the used lasers can have an effect on the intensities (Smith, Dent 2005). There were no or only minor peaks in the range above 1500 cm^{-1} since there were no aromatic structures in the cellulose sample.

The resonance enhancement of the minor amounts of aromatic structures in the UV range is depicted in Figure 29a.

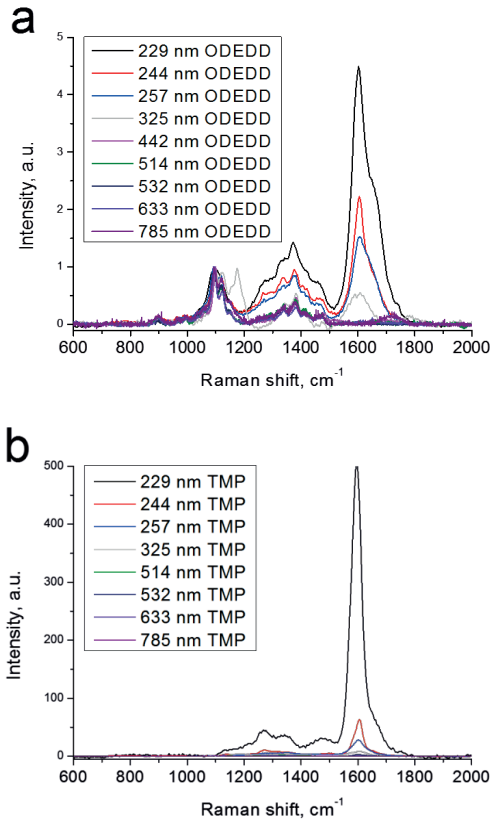

Figure 29. Raman spectra of a) bleached spruce kraft pulp (ODEDD) and b) spruce TMP (**Paper V**).

In Figure 29a, the Raman spectra of fully bleached spruce kraft pulp (ODEDD) with less than 0.1% lignin content (as measured from the kappa number) are illustrated as a function of laser excitation wavelength. The spectra had visible cellulose peaks at ca. 1095 cm^{-1} and also aromatic peaks at 1600 cm^{-1}. The aromatic peaks were very strong especially when measured with UV excitation, even though the kraft pulp was fully bleached, and the amount of lignin was small.

Figure 29b shows the Raman spectra of thermomechanical spruce fibers (TMP). Again, due to the high lignin content of the TMP, the aromatic peaks at 1600 cm^{-1} were extremely intense compared to the cellulose peaks at 1095 cm^{-1}. Regarding TMP, especially the UV excitation enhanced the aromatic bands quite considerably.

Figure 30 shows the Raman band intensities at 1600 cm^{-1} relative to 1095 cm^{-1} ($I_{1600\ cm^{-1}}$/ $I_{1095\ cm^{-1}}$) for all used excitation wavelengths and samples.

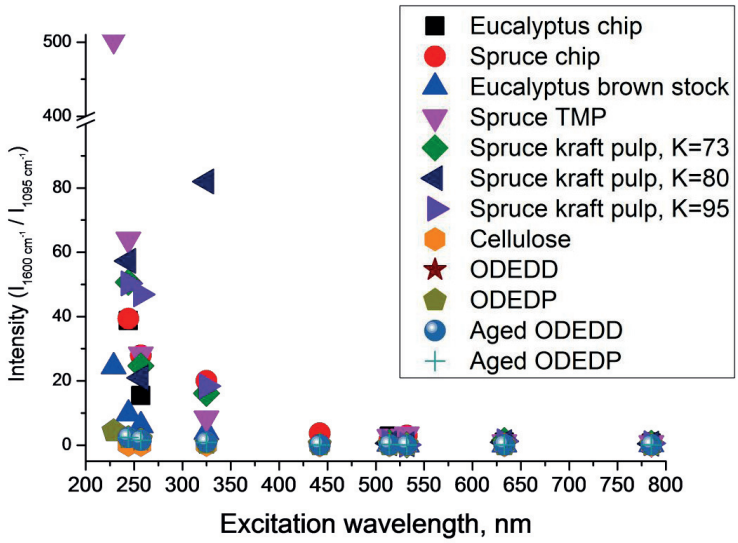

Figure 30. Intensity at 1600 cm^{-1} relative to 1095 cm^{-1} (**Paper V**).

Figure 30 shows how the relative heights of the aromatic peaks at 1600 cm^{-1} increased as the excitation wavelength was within UV region (257, 244 and 229 nm). For the kraft pulp samples, the resonance enhancement was strong already at 325 nm, and it increased to extremely strong for spruce TMP at lower wavelengths. The intensity value for spruce TMP was very high (ca. 500) when measured using excitation wavelength of 229 nm.

In order to observe the possible changes in the cellulose band area at ca. 1095/1120 cm^{-1}, the spectra were normalized also to the band at 1375 cm^{-1}. This band was chosen for the normalization in order to obtain information on the changes in cellulose bands regarding the extent of carbohydrate oxidation (Loureiro, Fernandes et al. 2011).

Furthermore, with this kind of normalization the aromatic peaks remained very strong when measured with UV excitation. However, as the band at 1375 cm^{-1} was normalized, the cellulose band intensity at 1095 cm^{-1} started increasing as the excitation wavelength became longer.

Figure 31a shows the Raman band intensities at 1600 cm^{-1} relative to 1095 cm^{-1} again for the selected cellulose, bleached spruce kraft pulp (ODEDD) and spruce TMP samples. In order to compare the two normalizations, Figure 31b shows the Raman band intensities at 1600 cm^{-1} relative to 1375 cm^{-1} for the same samples.

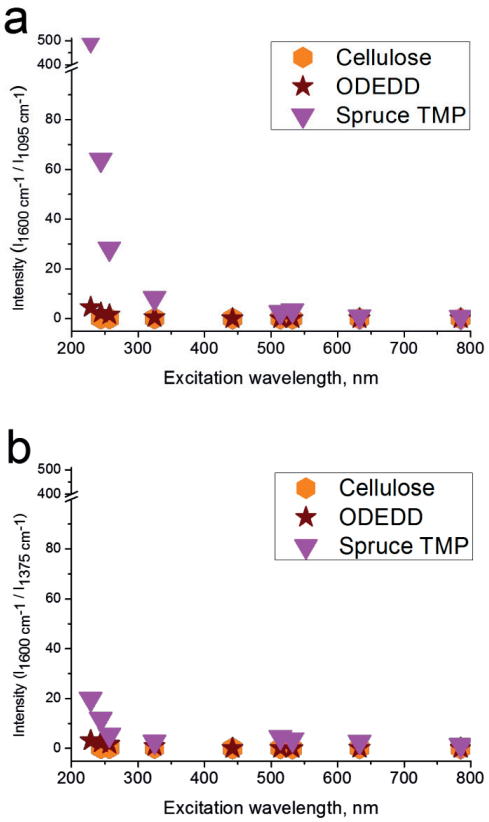

Figure 31. Intensity at 1600 cm^{-1} relative to intensity at a) 1095 cm^{-1} and b) 1375 cm^{-1} for cellulose, bleached spruce kraft pulp (ODEDD) and spruce TMP samples (**Paper V**).

When the two different normalizations in Figures 31a and 31b (normalization to the 1095 cm^{-1} band and to the 1375 cm^{-1} band) were compared, it could be seen that the resonance enhancement of the aromatic peak of spruce TMP at shorter excitation wavelengths showed a similar trend in both figures. However, the aromatic peak intensity of spruce TMP at 1600 cm^{-1} increased much less relative to the intensity at 1375 cm^{-1} than relative to the intensity at 1095 cm^{-1}. Thus it can be deduced that the intensity of the 1375 cm^{-1} band is also affected by the resonance enhancement of the aromatic band at 1600 cm^{-1} for short

excitation wavelengths in case of wood fibers (TMP) which have not been chemically treated. For bleached kraft pulp (ODEDD) and cellulose samples, no observable differences between the two normalizations were found (in Figures 31a and 31b).

Figure 32 shows the Raman band intensities at 1095 cm^{-1} relative to 1375 cm^{-1} for the same samples for a closer monitoring of the changes in the cellulose band.

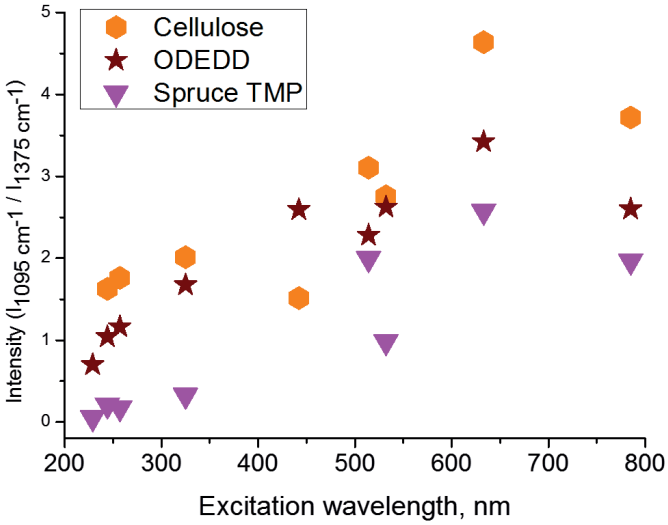

Figure 32. Intensity at 1095 cm^{-1} relative to intensity at 1375 cm^{-1} for cellulose, bleached spruce kraft pulp (ODEDD) and spruce TMP samples (**Paper V**).

When the normalization to the band at 1375 cm^{-1} was used, it was observed that the band at 1095 cm^{-1} was the most intense when the used excitation wavelength was 633 nm (Figure 32). The intensity was the smallest with UV excitation, and the band intensity increased as the excitation wavelength became longer, until the excitation was 633 nm. Interestingly, the excitation wavelength of 785 nm produced less intense band at 1095 cm^{-1}.

The results showed that the intensities of the characteristic vibration bands of different structural features depended on the excitation wavelength. With the correct laser frequency, it was possible to selectively enhance individual groups in the molecule. Even if this phenomenon has been observed with model compounds and other biological

materials, it has not been widely exploited when analyzing the Raman spectra of pulp and wood samples.

In the spectra collected at 229, 244 and 257 nm, the aromatic band intensity was much stronger than in the spectra measured using higher wavelengths for all samples. However, regarding kraft pulp samples, the resonance enhancement was strong already at 325 nm, and it increased to extremely strong for spruce TMP at lower wavelengths.

6 Concluding remarks

In the analysis of spruce kraft pulps the height of the lignin band in the UV-Vis spectra (280 nm) correlated well with the lignin band in the UVRR spectra (1605 cm^{-1}) for semi- or fully-bleached pulps. However, the correlation was much weaker for unbleached pulps. Furthermore, the results for hexenuronic acid content by UV-Vis (240 nm) and UVRR (1658 cm^{-1}) methods correlated well for most of the pulps, but for unbleached or peroxide-bleached samples the interference from other structures affecting these bands was obvious. Nevertheless, UV resonance Raman spectroscopy was shown to be a valuable technique in lignin analysis *in situ*, especially for pulp samples with a low lignin content.

The changes in the lignin structure of spruce thermomechanical pulp (TMP), induced by the treatment with laccase of *Trametes hirsuta* (ThL) and laccase of *Melanocarpus albomyces* (MaL), was investigated by UV resonance Raman (UVRR), UV-Vis, and Fourier transform infrared (FTIR) spectroscopies. The spectroscopic results showed that the structural changes were small. However, the changes were slightly more pronounced in the case of MaL. Monitoring small changes in TMP samples with a high lignin content using Raman spectroscopy proved to be challenging, as the resonance enhancement of aromatic band became very strong.

Ultraviolet resonance Raman (UVRR) spectroscopy was proven to be a powerful tool for structural lignin analysis *in situ*: the modification or isolation of lignin from biomass was not necessary. UVRR spectroscopy was equally applicable to samples with a high lignin content and those with a very low lignin content. Monomeric phenolic lignin model compounds and wood pulp samples were studied at neutral and alkaline pH with UVRR spectroscopy. Concentration of guaiacol correlated well with the relative Raman band intensity, which indicated that the lignin containing solutions can be quantitatively measured with UVRR spectroscopy. A change in pH induced a recordable shift in the aromatic band position in the spectra, which was 25-35 cm^{-1} with phenolic model compounds without *para* substitution, 8-12 cm^{-1} with phenolic model compounds with *para* substitution, and about 2-7 cm^{-1} with pulp samples. No shift was detected with a non-phenolic model compound. Increasing the amount of phenolic hydroxyl groups increased the UVRR band shift in pulp samples. Additionally, increasing the pH enhanced the relative aromatic band intensity in the UVRR spectra in solution of the phenolic model compound. Accordingly, the pH adjustment was shown to be relevant prior to any lignin analysis with Raman spectroscopy.

Raman spectroscopy of lignin-containing samples may produce laser induced fluorescence (LIF) which overlaps with Raman bands. This background signal can, in the worst case, overwhelm the weaker Raman signal completely and, hence, obstruct the sample characterization. Lignin model compounds containing a biphenyl structure exhibited strong laser induced fluorescence with visible 532 nm excitation in Raman spectroscopy. By comparing the Raman spectra from various lignin model compounds, the source of fluorescence emission was concluded to be the 5-5' linkage. The effect of 5-5' linkage on laser induced fluorescence is seen in the spectra of erol and bierol, as the former produced a very clear Raman signal, and the latter was fluorescing intensively. Dibenzodioxocin also contained the 5-5' linkage, but it was not fluorescing at 532 nm, likely due to an effect of its eight-membered ring structure on fluorescence.

Wood did not emit laser induced fluorescence with visible 532 nm excitation. Lignin was in its native form and surrounded by the wood matrix that has an effect on fluorescence properties. When wood was chemically treated under alkaline conditions, lignin was cleaved and started to emit fluorescence. The most easily breaking structures were the α- and β-aryl ether structures in dibenzodioxocin, whereas the 5-5' linkages as such were not cleaved. The Raman spectroscopic study of MWL and EMAL showed that the laser induced fluorescence emission was overwhelming in their Raman spectra. The synthetically prepared DHP lignin produced a relatively clear Raman signal similar to the Raman signal of spruce wood and, thus, was shown not to act as a complete model for native lignin.

The intensities of the characteristic vibration bands of different structural features in the Raman spectra of wood-based biomass were shown to depend on the excitation wavelength. With correct laser frequency, it was possible to selectively enhance individual groups in the molecule. Even if this phenomenon had been observed with model compounds and other biological materials before, it had not been widely exploited when analyzing the Raman spectra of pulp and wood samples.

The UV light used in excitation enhanced the signals arising from the aromatic and unsaturated structures by several orders of magnitude. Although the resonance enhancement of the aromatic structures can cause challenges in the analysis of TMP or even unbleached pulps, Raman spectroscopy using UV excitation is a very sensitive tool as it reveals information on even small amounts of aromatic structures.

7 References

ADLER, E. and HERNESTAM, S., 1955. Estimation of phenolic hydroxyl groups in lignin. *Acta Chem.Scand,* **9**(2), pp. 319-334.

ADORJAN, I., JÄÄSKELÄINEN, A.-S. and VUORINEN, T., 2006. Synthesis and characterization of the hexenuronic acid model methyl 4-deoxy-β-l-threo-hex-4-enopyranosiduronic acid. *Carbohydrate research,* **341**(14), pp. 2439-2443.

AGARWAL, U.P., 1999. An overview of Raman spectroscopy as applied to lignocellulosic materials. In: D.S. ARGYROPOULOS, ed, *Advances in lignocellulosics characterization.* Atlanta, GA: Tappi Press, pp. 201-225.

AGARWAL, U.P. and ATALLA, R.H., 1986. In-situ Raman microprobe studies of plant cell walls: macromolecular organization and compositional variability in the secondary wall of Picea mariana (Mill.) BSP. *Planta,* **169**(3), pp. 325-332.

AGARWAL, U.P. and RALPH, S.A., 2008. Determination of ethylenic residues in wood and TMP of spruce by FT-Raman spectroscopy. *Holzforschung,* **62**(6), pp. 667-675.

AGARWAL, U.P. and TERASHIMA, N., 2003. FT-Raman study of dehydrogenation polymer (DHP) lignins, *12th ISWPC International Symposium on Wood and Pulping Chemistry, Madison, Wisconsin, USA*, June 9-12 2003.

ATALLA, R.H. and AGARWAL, U.P., 1985. Raman microprobe evidence for lignin orientation in the cell walls of native woody tissue. *Science,* **227**(4687), pp. 636-638.

BALAKSHIN, M., CAPANEMA, E., GRACZ, H., CHANG, H. and JAMEEL, H., 2011. Quantification of lignin–carbohydrate linkages with high-resolution NMR spectroscopy. *Planta,* **233**(6), pp. 1097-1110.

BARCLAY, L.R.C., XI, F. and NORRIS, J.Q., 1997. Antioxidant properties of phenolic lignin model compounds. *Journal of Wood Chemistry and Technology,* **17**(1-2), pp. 73-90.

BARSBERG, S., MATOUSEK, P. and TOWRIE, M., 2005. Structural analysis of lignin by resonance raman spectroscopy. *Macromolecular bioscience,* **5**(8), pp. 743-752.

BARSBERG, S., MATOUSEK, P., TOWRIE, M., JØRGENSEN, H. and FELBY, C., 2006. Lignin radicals in the plant cell wall probed by Kerr-gated resonance Raman spectroscopy. *Biophysical journal,* **90**(8), pp. 2978-2986.

BOERJAN, W., RALPH, J. and BAUCHER, M., 2003. Lignin biosynthesis. *Annual Review of Plant Biology,* **54**(1), pp. 519-546.

BOUDET, A., LAPIERRE, C. and GRIMA-PETTENATI, J., 1995. Tansley review No. 80. Biochemistry and molecular biology of lignification. *New Phytologist,* , pp. 203-236.

BRAHMA, S.K., HARGRAVES, P.E., HOWARD, W.F. and NELSON, W.H., 1983. Resonance Raman method for the rapid detection and identification of algae in water. *Applied Spectroscopy,* **37**(1), pp. 55-58.

BROWN, S.B., 1980. *An Introduction to spectroscopy for biochemists*. London, UK: Academic Press.

BRUNOW, G., 2001. Methods to reveal the structure of lignin. In: M. HOFRICHTER and A. STEINBÜCHEL, eds, *Biopolymers. Volume 1, Lignin, humic substances and coal.* Weinheim: Wiley-VCH, pp. 89-116.

BUCHERT, J., MUSTRANTA, A., TAMMINEN, T., SPETZ, P. and HOLMBOM, B., 2002. Modification of spruce lignans with Trametes hirsuta laccase. *Holzforschung,* **56**(6), pp. 579-584.

CAPANEMA, E.A., BALAKSHIN, M.Y. and KADLA, J.F., 2004. A comprehensive approach for quantitative lignin characterization by NMR spectroscopy. *Journal of Agricultural and Food Chemistry,* **52**(7), pp. 1850-1860.

CHANDRA, R.P., BEATSON, R.P., DE JONG, E. and SADDLER, J.N., 1999. Effects of treatment with the white-rot fungus Trametes versicolor and laccase enzymes on the brightness of Douglas-fir heartwood derived thermomechanical pulps. *Journal of Wood Chemistry and Technology,* **19**(1), pp. 61-78.

CHI, Z., CHEN, X., HOLTZ, J.S.W. and ASHER, S.A., 1998. UV resonance Raman-selective amide vibrational enhancement: quantitative methodology for determining protein secondary structure. *Biochemistry,* **37**(9), pp. 2854-2864.

CLAUS, H., 2004. Laccases: Structure, reactions, distribution. *Micron,* **35**(1-2), pp. 93-96.

CLAUS, H., 2003. Laccases and their occurrence in prokaryotes. *Archives of Microbiology,* **179**(3), pp. 145-150.

CONNERS, T.E., 1995. *Surface analysis of paper.* Boca Raton, FL: CRC Press.

DEL RÍO, J.C., GUTIÉRREZ, A., HERNANDO, M., LANDÍN, P., ROMERO, J. and MARTÍNEZ, ÁT., 2005. Determining the influence of eucalypt lignin composition in paper pulp yield using Py-GC/MS. *Journal of Analytical and Applied Pyrolysis,* **74**(1), pp. 110-115.

DELMAS, D., LACHENAL, D., MORTHA, G., MARLIN, N. and CALAIS, C., 2009. Titration of free phenolic groups in pulps. *Holzforschung,* **63**(6), pp. 705-710.

DIZHBITE, T., TELYSHEVA, G., JURKJANE, V. and VIESTURS, U., 2004. Characterization of the radical scavenging activity of lignins––natural antioxidants. *Bioresource technology,* **95**(3), pp. 309-317.

DOHERTY, W.O.S., MOUSAVIOUN, P. and FELLOWS, C.M., 2011. Value-adding to cellulosic ethanol: Lignin polymers. *Industrial Crops and Products,* **33**(2), pp. 259-276.

ESHKIKI, R.B., MORTHA, G. and LACHENAL, D., 2007. A new method for the titration of free phenolic groups in pulps. *Holzforschung,* **61**(3), pp. 242-246.

FELBY, C., PEDERSEN, L.S. and NIELSEN, B.R., 1997. Enhanced auto adhesion of wood fibers using phenol oxidases. *Holzforschung,* **51**(3), pp. 281-286.

FENGEL, D. and WEGENER, G., 1984. *Wood: chemistry, ultrastructure, reactions*. München, Germany: Verlag Kessel.

FESSENDEN, R.J. and FESSENDEN, J.S., 1994. *Organic chemistry*. 5th ed. edn. Pacific Grove (CA): Brooks/Cole.

FORSS, K.G. and FREMER, K.E., 2003. *The Nature and Reactions of Lignin: A New Paradigm*. Helsinki, Finland: the authors.

FROASS, P.M., RAGAUSKAS, A.J. and JIANG, J., 1996. Chemical structure of residual lignin from kraft pulp. *Journal of Wood Chemistry and Technology,* **16**(4), pp. 347-365.

FUJIMOTO, A., MATSUMOTO, Y., CHANG, H.M. and MESHITSUKA, G., 2005. Quantitative evaluation of milling effects on lignin structure during the isolation process of milled wood lignin. *Journal of Wood Science,* **51**(1), pp. 89-91.

GELLERSTEDT, G. and LINDFORS, E., 1984. Structural changes in lignin during kraft cooking. Part 4. Phenolic hydroxyl groups in wood and kraft pulps. *Svensk Papperstidn.,* **87**(15), pp. R115-R118.

GIERLINGER, N. and SCHWANNINGER, M., 2007. The potential of Raman microscopy and Raman imaging in plant research. *Spectroscopy,* **21**(2), pp. 69-89.

GLASSER, W.G., NORTHEY, R.A. and SCHULTZ, T.P., 2000. *Lignin : historical, biological, and materials perspectives*. Washington, D.C: American Chemical Society.

GRÖNQVIST, S., RANTANEN, K., ALÉN, R., MATTINEN, M.-L., BUCHERT, J. and VIIKARI, L., 2006. Laccase-catalysed functionalisation of TMP with tyramine. *Holzforschung,* **60**(5), pp. 503-508.

GRÖNQVIST, S., VIIKARI, L., NIKU-PAAVOLA, M.-L., ORLANDI, M., CANEVALI, C. and BUCHERT, J., 2005. Oxidation of milled wood lignin with laccase, tyrosinase and horseradish peroxidase. *Applied Microbiology and Biotechnology,* **67**(4), pp. 489-494.

GRÖNQVIST, S., BUCHERT, J., RANTANEN, K., VIIKARI, L. and SUURNÄKKI, A., 2003. Activity of laccase on unbleached and bleached thermomechanical pulp. *Enzyme and microbial technology,* **32**(3-4), pp. 439-445.

HALTTUNEN, M., VYÖRYKKÄ, J., HORTLING, B., TAMMINEN, T., BATCHELDER, D., ZIMMERMANN, A. and VUORINEN, T., 2001. Study of residual lignin in pulp by UV resonance Raman spectroscopy. *Holzforschung,* **55**(6), pp. 631-638.

HEARLE, J., 1963. The fine structure of fibers and crystalline polymers. I. Fringed fibril structure. *Journal of Applied Polymer Science,* **7**(4), pp. 1175-1192.

JÄÄSKELÄINEN, A.-S., SAARIAHO, A.-M. and VUORINEN, T., 2005. Quantification of lignin and hexenuronic acid in bleached hardwood kraft pulps: A new calibration method for UVRR spectroscopy and evaluation of the conventional methods. *Journal of Wood Chemistry and Technology,* **25**(1-2), pp. 51-65.

JOHANSSON, L.S., CAMPBELL, J., KOLJONEN, K. and STENIUS, P., 1999. Evaluation of surface lignin on cellulose fibers with XPS. *Applied Surface Science,* **144**, pp. 92-95.

KARHUNEN, P., RUMMAKKO, P., SIPILÄ, J., BRUNOW, G. and KILPELÄINEN, I., 1995. Dibenzodioxocins; a novel type of linkage in softwood lignins. *Tetrahedron letters,* **36**(1), pp. 169-170.

KIISKINEN, L.-L., VIIKARI, L. and KRUUS, K., 2002. Purification and characterisation of a novel laccase from the ascomycete Melanocarpus albomyces. *Applied Microbiology and Biotechnology,* **59**(2-3), pp. 198-204.

KLEEN, M., KANGAS, H. and LAINE, C., 2003. Chemical characterization of mechanical pulp fines and fiber surface layers. *Nordic Pulp and Paper Research Journal,* **18**(4), pp. 361-368.

KONTTURI, E., SUCHY, M., PENTTILÄ, P., JEAN, B., PIRKKALAINEN, K., TORKKELI, M. and SERIMAA, R., 2011. Amorphous Characteristics of an Ultrathin Cellulose Film. *Biomacromolecules,* (12), pp. 770-777.

LÄHDETIE, A., LIITIÄ, T., TAMMINEN, T. and JÄÄSKELÄINEN, A.-S., 2009. Reflectance UV-Vis and UV resonance Raman spectroscopy in characterization of kraft pulps. *BioResources,* **4**(4), pp. 1600-1619.

LÄHDETIE, A., LIITIÄ, T., TAMMINEN, T., JÄÄSKELÄINEN, A.-S., DELMAS, D. and MORTHA, G., 2007. Comparison of phenolic hydroxyl group determination methods, *COST Action E41 Workshop: "Functional Groups and Surface Analysis of Wood and Fibres", Rome, Italy*, May 7-8 2007, pp. 7-8.

LÄHDETIE, A., LIITIÄ, T., TAMMINEN, T., PERE, J. and JÄÄSKELÄINEN, A.-S., 2009. Activation of thermomechanical pulp by laccases as studied by UV-Vis, UV resonance Raman and FTIR spectroscopy. *Holzforschung,* **63**(6), pp. 745-750.

LAKOWICZ, J.R. and MASTERS, B.R., 2008. *Principles of fluorescence spectroscopy*. New York, NY: Springer.

LAPIERRE, C., POLLET, B., PETIT-CONIL, M., TOVAL, G., ROMERO, J., PILATE, G., LEPLÉ, J.C., BOERJAN, W., FERRET, V. and DE NADAI, V., 1999. Structural Alterations of Lignins in Transgenic Poplars with Depressed Cinnamyl Alcohol Dehydrogenase or Caffeic AcidO-Methyltransferase Activity Have an Opposite Impact on the Efficiency of Industrial Kraft Pulping. *Plant Physiology,* **119**(1), pp. 153-164.

LARSEN, K.L. and BARSBERG, S., 2010. Theoretical and Raman Spectroscopic Studies of Phenolic Lignin Model Monomers. *The Journal of Physical Chemistry B,* **114**(23), pp. 8009-8021.

LIITIÄ, T., RANUA, M., OHRA-AHO, T., HORTLING, B., PEKKALA, O. and TAMMINEN, T., 2005. Formation of chromophores during alkaline pulping: Effects on bleachability and brightness stability, *The International Pulp Bleaching Conference, Stockholm, Sweden*, June 14–16 2005, pp. 194-199.

LIITIÄ, T. and TAMMINEN, T., 2007. Direct method for the determination of phenolic hydroxyl groups in pulp. *Holzforschung,* **61**(6), pp. 623-627.

LIITIÄ, T., TAMMINEN, T. and RANUA, M., 2004. Chemistry of bleaching elucidated by UV-VIS reflectance spectroscopy, *Proceedings of the 8th European Workshop on Lignocellulosics and Pulp, Riga, Latvia*, August 22-25 2004, pp. 247-250.

LIN, S.Y. and DENCE, C.W., 1992. *Methods in lignin chemistry*. Berlin, Germany: Springer.

LOUREIRO, P.E.G., FERNANDES, A.J.S., FURTADO, F.P., CARVALHO, M. and EVTUGUIN, D.V., 2011. UV-resonance Raman micro-spectroscopy to assess residual chromophores in cellulosic pulps. *Journal of Raman Spectroscopy,* **42**(5), pp. 1039-1045.

LUUKKO, K., 1998. On the characterization of mechanical pulp fines: A review. *Paperi ja Puu/Paper and Timber,* **80**(6), pp. 441-448.

MARK, H., 1940. Intermicellar Hole and Tube System in Fiber Structure. *The Journal of physical chemistry,* **44**(6), pp. 764-788.

MATOUSEK, P., TOWRIE, M., MA, C., KWOK, W., PHILLIPS, D., TONER, W. and PARKER, A., 2001. Fluorescence suppression in resonance Raman spectroscopy using a high-performance picosecond Kerr gate. *Journal of Raman Spectroscopy,* **32**(12), pp. 983-988.

MATOUSEK, P., TOWRIE, M., STANLEY, A. and PARKER, A., 1999. Efficient rejection of fluorescence from Raman spectra using picosecond Kerr gating. *Applied Spectroscopy,* **53**(12), pp. 1485-1489.

MCCREERY, R.L., 2000. *Raman spectroscopy for chemical analysis*. USA: John Wiley & Sons, Inc.

MEYER, M.W., LUPOI, J.S. and SMITH, E.A., 2011. 1064 nm dispersive multichannel Raman spectroscopy for the analysis of plant lignin. *Analytica Chimica Acta,* .

NIKU-PAAVOLA, M.-L., KARHUNEN, E., SALOLA, P. and RAUNIO, V., 1988. Ligninolytic enzymes of the white-rot fungus Phlebia radiata. *Biochemical Journal,* **254**(3), pp. 877-884.

NIKU-PAAVOLA, M.-L., TAMMINEN, T., HORTLING, B., VIIKARI, L. and POPPIUS-LEVLIN, K., 2002. Reactivity of high and low molar mass lignin in the laccase catalysed oxidation. *Progress in Biotechnology,* **21**, pp. 121-130.

NUOPPONEN, M., WILLFÖR, S., JÄÄSKELÄINEN, A.-S., SUNDBERG, A. and VUORINEN, T., 2004. A UV resonance Raman (UVRR) spectroscopic study on the extractable compounds of Scots pine (Pinus sylvestris) wood: Part I: Lipophilic compounds. *Spectrochimica Acta - Part A: Molecular and Biomolecular Spectroscopy,* **60**(13), pp. 2953-2961.

NUOPPONEN, M., 2005. *FT-IR and UV Raman spectroscopic studies on thermal modification of scots pine wood and its extractable compounds*. Espoo, Finland: Helsinki University of Technology.

ORBLIN, E. and FARDIM, P., 2010. Surface chemistry of deinked pulps as analysed by XPS and ToF-SIMS. *Surface and Interface Analysis,* **42**(12-13), pp. 1712-1722.

PANDEY, K.K. and VUORINEN, T., 2008. Comparative study of photodegradation of wood by a UV laser and a xenon light source. *Polymer Degradation and Stability,* **93**(12), pp. 2138-2146.

PELLETIER, M.J., 1999. *Analytical applications of Raman spectroscopy*. Cornwall, Great Britain: Wiley-Blackwell.

PELLETIER, M., 2003. Quantitative analysis using Raman spectrometry. *Applied Spectroscopy,* **57**(1), pp. 20-20.

PETIT-CONIL, M., SEMAR, S., NIKU-PAAVOLA, M.-L., SIGOILLOT, J.C., ASTHER, M., ANKE, H. and VIIKARI, L., 2002. Potential of laccases in softwood-hardwood high-yield pulping and bleaching. *Progress in Biotechnology,* **21**, pp. 193-201.

RAGNAR, M., 2001. A novel spectrophotometric tool for bleaching studies and determination of hexenuronic acid removal. *Nordic Pulp and Paper Research Journal,* **16**(1), pp. 68-71.

RAMAN, C.V. and KRISHNAN, K., 1928. A new type of secondary radiation. *Nature,* **121**(3048), pp. 501-502.

RITTSTIEG, K., SUURNAKKI, A., SUORTTI, T., KRUUS, K., GUEBITZ, G. and BUCHERT, J., 2002. Investigations on the laccase-catalyzed polymerization of lignin model compounds using size-exclusion HPLC. *Enzyme and microbial technology,* **31**(4), pp. 403-410.

SAARIAHO, A.-M., ARGYROPOULOS, D.S., JÄÄSKELÄINEN, A.-S. and VUORINEN, T., 2005. Development of the partial least squares models for the interpretation of the UV resonance Raman spectra of lignin model compounds. *Vibrational Spectroscopy,* **37**(1), pp. 111-121.

SAARIAHO, A.-M., HORTLING, B., JÄÄSKELÄINEN, A.-S., TAMMINEN, T. and VUORINEN, T., 2003. Simultaneous Quantification of Residual Lignin and Hexenuronic Acid from Chemical Pulps with UV Resonance Raman Spectroscopy and Multivariate Calibration. *Journal of Pulp and Paper Science,* **29**(11), pp. 363-370.

SAARIAHO, A.-M., JÄÄSKELÄINEN, A.-S., MATOUSEK, P., TOWRIE, M., PARKER, A.W. and VUORINEN, T., 2004. Resonance Raman spectroscopy of highly fluorescing lignin containing chemical pulps: Suppression of fluorescence with an optical Kerr gate. *Holzforschung,* **58**(1), pp. 82-90.

SAARIAHO, A.-M., JÄÄSKELÄINEN, A.-S., NUOPPONEN, M. and VUORINEN, T., 2003. Ultra violet resonance Raman spectroscopy in lignin analysis: Determination of characteristic vibrations of p-hydroxyphenyl, guaiacyl, and syringyl lignin structures. *Applied Spectroscopy,* **57**(1), pp. 58-66.

SAARINEN, T., SUURNÄKKI, A., ÖSTERBERG, M. and LAINE, J., 2009. Modification of lignin with laccases for the adsorption of anionic ferulic acid studied by quartz cristall microbalance with dissipation and AFM. *Holzforschung,* **63**(3), pp. 298-306.

SCALLAN, A., 1971. A quantitative picture of the fringed micellar model of cellulose. *Textile Research Journal,* **41**(8), pp. 647-652.

SCHMIDT, J. and HEITNER, C., 1999. Use of diffuse reflectance UV-visible spectroscopy to characterize chromophores in wood fibers. In: D.S. ARGYROPOULOS, ed, *Advances in Lignocellulosics Characterization*. Atlanta, GA: Tappi Press, pp. 179-199.

SCHULZ, H. and BARANSKA, M., 2007. Identification and quantification of valuable plant substances by IR and Raman spectroscopy. *Vibrational spectroscopy,* **43**(1), pp. 13-25.

SJÖSTRÖM, E. and ALEN, R., 1999. *Analytical methods in wood chemistry, pulping, and papermaking*. Berlin Heidelberg, Germany: Springer Verlag.

SMITH, E. and DENT, G., 2005. *Modern Raman spectroscopy : a practical approach*. Chichester: Wiley.

STENIUS, P., ed, 2000. *Book 3: Forest products chemistry*. Jyväskylä, Finland: Fapet Oy.

SUNDHOLM, J., 1999. *Book 5: Mechanical pulping*. Jyväskylä, Finland: Fapet Oy.

TAMMINEN, T., LIITIÄ, T., OHRA-AHO, T. and HORTLING, B., 2004. Do we need to isolate pulp residual lignin for its structural characterization, *8th European Workshop of Lignocellulosics and Pulp, Riga, Latvia*, August 22-25 2004, pp. 37-40.

TELEMAN, A., HARJUNPÄÄ, V., TENKANEN, M., BUCHERT, J., HAUSALO, T., DRAKENBERG, T. and VUORINEN, T., 1995. Characterisation of acid attached to xylan in pine kraft pulp and pulping liquor by 1H and 13C NMR spectroscopy. *Carbohydrate research,* **272**(1), pp. 55-71.

VUORINEN, T., ADORJAN, I., JÄÄSKELÄINEN, A.-S., LEHTIMAA, T., TOIKKA, K. and ZHOU, Z., 2007. Reactivity of hexenuronic acid in bleaching of eucalyptus kraft pulps, *3rd International Colloquium on Eucalyptus Pulp, Belo Horizonte, Brazil*, March 4-7 2007.

WARSTA, E., JÄÄSKELÄINEN, A.-S., VUORINEN, T. and PITKÄNEN, M., 2006. Direct determination of phenolic hydroxyl groups with UV-resonance raman spectroscopy, *9 th European Workshop of Lignocellulosics and Pulp, Vienna, Austria*, August 27-30 2006, pp. 572-574.

WILEY, J.H. and ATALLA, R.H., 1987. Band assignments in the Raman spectra of celluloses. *Carbohydrate research,* **160**, pp. 113-129.

WU, Q., NELSON, W., TREUBIG JR, J., BROWN, P., HARGRAVES, P., KIRS, M., FELD, M., DESARI, R., MANOHARAN, R. and HANLON, E., 2000. UV resonance Raman detection and quantitation of domoic acid in phytoplankton. *Analytical Chemistry,* **72**(7), pp. 1666-1671.

ZAKIS, G.F., 1994. *Functional analysis of lignins and their derivatives*. Atlanta, GA: Tappi Press.

ZAKZESKI, J., BRUIJNINCX, P.C.A. and WECKHUYSEN, B.M., 2011. *In situ* spectroscopic investigation of the cobalt-catalyzed oxidation of lignin model compounds in ionic liquids. *Green Chem.,* (13), pp. 671-680.

ZOUBIR, A., ed, 2012. *Raman Imaging*. Berlin Heidelberg: Springer.

Aalto-DD 202/2013

ISBN 978-952-60-5468-1
ISBN 978-952-60-5469-8 (pdf)
ISSN-L 1799-4934
ISSN 1799-4934
ISSN 1799-4942 (pdf)

Aalto University
School of Chemical Technology
Department of Forest Products Technology
www.aalto.fi

BUSINESS +
ECONOMY

ART +
DESIGN +
ARCHITECTURE

SCIENCE +
TECHNOLOGY

CROSSOVER

DOCTORAL
DISSERTATIONS